

# Structured Shrinkage Priors

Maryclare Griffin\*

Center for Applied Mathematics, Cornell University,  
Ithaca, NY 14853, USA

and

Peter D. Hoff

Department of Statistical Science, Duke University,  
Durham, NC 27710, USA

November 10, 2021

## Abstract

In many regression settings the unknown coefficients may have some known structure, for instance they may be ordered in space or correspond to a vectorized matrix or tensor. At the same time, the unknown coefficients may be sparse, with many nearly or exactly equal to zero. However, many commonly used priors and corresponding penalties for coefficients do not encourage simultaneously structured and sparse estimates. In this paper we develop structured shrinkage priors that generalize multivariate normal, Laplace, exponential power and normal-gamma priors. These priors allow the regression coefficients to be correlated a priori without sacrificing element-wise sparsity or shrinkage. The primary challenges in working with these structured shrinkage priors are computational, as the corresponding penalties are intractable integrals and the full conditional distributions that are needed to approximate the posterior mode or simulate from the posterior distribution may be non-standard. We overcome these issues using a flexible elliptical slice sampling procedure, and demonstrate that these priors can be used to introduce structure while preserving sparsity of the corresponding penalized estimate given by the posterior mode.

*Keywords: Bayesian lasso, Lasso, multivariate Laplace, multivariate normal-scale mixture, sparsity, shrinkage.*

---

\*Corresponding author. Email address: maryclare@cornell.edu

# 1 Introduction

Shrinkage prior-based penalized estimates of regression coefficients are ubiquitous and useful for good reason. When we observe an  $n \times 1$  vector of responses  $\mathbf{y}$  and an  $n \times p$  matrix of regressors  $\mathbf{X}$  and the data are high dimensional, i.e. the number of covariates  $p$  is large relative to the number of responses  $n$ , traditional regression methods can fail. They may produce estimates of the  $p \times 1$  vector of regression coefficients  $\boldsymbol{\beta}$  have prohibitively large variance or are not unique because the data provide relatively little information about the unknown regression coefficients.

Using a prior for  $\boldsymbol{\beta}$  that reflects our *a priori* knowledge of the problem, we can obtain better estimates of  $\boldsymbol{\beta}$ . When our *a priori* knowledge involves similarities and differences among elements of  $\boldsymbol{\beta}$ , we might assume a structured mean-zero multivariate normal prior with covariance matrix  $\boldsymbol{\Sigma}$ . Alternatively, when our *a priori* knowledge involves relative magnitudes of elements of  $\boldsymbol{\beta}$ , we might assume a sparsity inducing mean-zero independent Laplace prior with variance  $\sigma^2$  in order to encode information about the origin and tail behavior of  $\boldsymbol{\beta}$ . This is especially useful when  $\boldsymbol{\beta}$  is expected to be sparse, as the posterior mode of  $\boldsymbol{\beta}$  under a mean-zero independent Laplace prior corresponds to the  $\ell_1$  or lasso penalized estimate of  $\boldsymbol{\beta}$  (Tibshirani, 1996; Park and Casella, 2008).

When our *a priori* knowledge involves both similarities and differences among and relative magnitudes of elements of  $\boldsymbol{\beta}$ , it would be desirable to assume a structured sparsity inducing shrinkage prior. As an example, consider the analysis of brain-computer interface data. Brain-computer interfaces (BCIs) are used to detect changes in subjects' cognitive state from contemporaneous electroencephalography (EEG) measurements, which can be collected non-invasively at high temporal resolution (Makeig et al., 2012; Wolpaw and Wolpaw, 2012). We consider the P300 speller, a specific BCI device which is designed to detect when a subject is viewing a specified target letter (Forney et al., 2013). For an individual subject, we observe 240 indicators  $y_i$  for whether or not the subject was viewing a specified target letter during trial  $i$ , and  $\mathbf{x}_i$  is a vectorized  $208 \times 8$  matrix of EEG measurements from  $p_1 = 208$  time points and  $p_2 = 8$  channels. The corresponding vector of regression coefficients is likewise a vectorized  $208 \times 8$  matrix,  $\boldsymbol{\beta} = \text{vec}(\mathbf{B})$ . Figure 1a shows data from a single subject and a subset of trials, and Figure 1b shows the eight

distinct physical locations on the top of the skull. Scientifically, we expect to observe a P300 wave during trials when the target letter is present, which is characterized by a sharp rise and then dip before returning to equilibrium. We expect that the wave will begin shortly after the target letter is shown, and will be observed earlier and more clearly on some channels than others. That said, EEG data are notoriously noisy and the P300 wave is difficult to observe in the data. Fortunately, the scientific context suggests that the unobserved regression coefficients  $\mathbf{B}$  should be sparse and structured, as only elements of  $\mathbf{B}$  that correspond to time points where the P300 wave occurs are expected to be nonzero and elements of  $\mathbf{B}$  corresponding to consecutive time points or neighboring channels are expected to be similar.

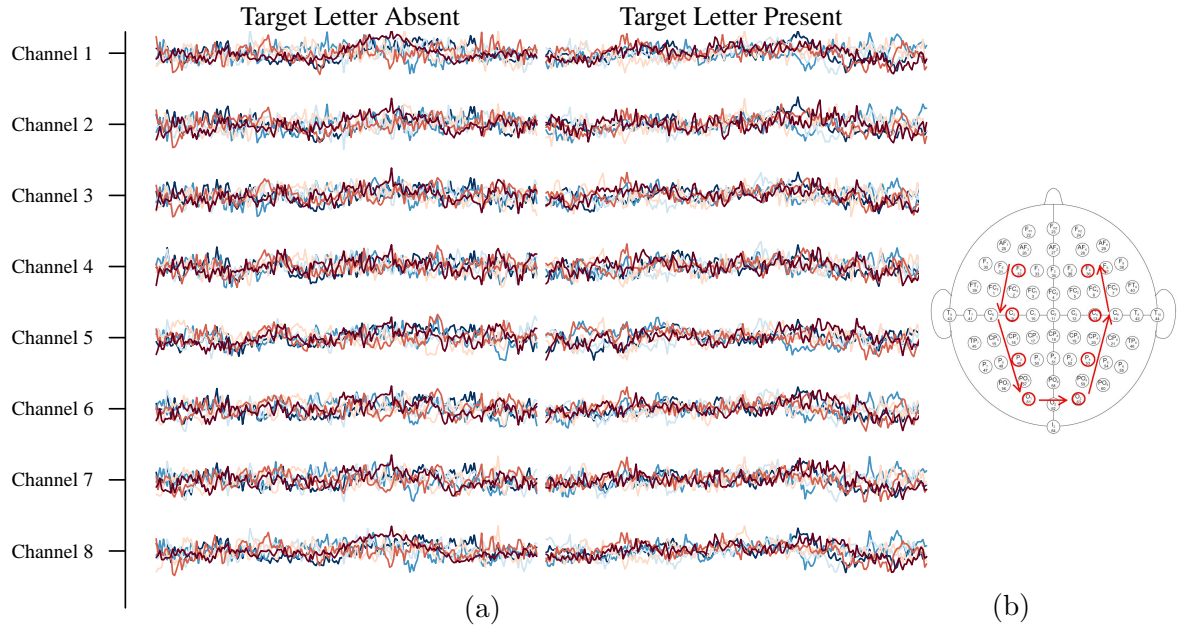


Figure 1: Panel (a) shows a subset of single-subject P300 speller data. Lines represents trials, i.e. rows  $\mathbf{x}_i$ . Trials are plotted separately by whether or not the target letter was being shown during the trial. Panel (b) shows the locations of EEG sensors on the skull reprinted and modified from Sharma (2013), with sensors included in our analysis highlighted in red. Arrows indicate the order of the channels as they appear in the data.

In such settings, we would like to work with a class of structured shrinkage priors that (i) can incorporate *a priori* knowledge of structure by allowing elements of  $\boldsymbol{\beta}$  to covary with nondiagonal prior covariance matrix  $\boldsymbol{\Sigma} = \mathbb{V}[\boldsymbol{\beta}]$ , (ii) can incorporate *a priori* knowledge of

sparsity by allowing elementwise shrinkage of  $\beta$  and a possibly sparse posterior mode, and (iii) span the range of common structured and sparsity inducing priors by generalizing the multivariate normal prior as well as the independent Laplace prior. However, existing approaches fail to satisfy all three of these criteria.

We can see this by considering the normal scale-mixture representations of many common priors, which are used in most Bayesian approaches to sparse regression (Polson and Scott, 2010). Letting ‘ $\circ$ ’ be the Hadamard elementwise product,  $\mathbf{z} \sim \text{normal}(\mathbf{0}, \mathbf{\Omega})$  and  $\mathbf{s}$  be a vector of stochastic scales that are independent of  $\mathbf{z}$ , a prior distribution for  $\beta$  has a normal scale-mixture representation if there exists a density  $p(\mathbf{s}|\theta)$  such that  $\beta \stackrel{d}{=} \mathbf{s} \circ \mathbf{z}$ . These priors are easy to interpret from a data generating perspective and have easy-to-compute moments. Specifically the prior covariance matrix of  $\beta$  that encodes the *a priori* knowledge of structure is  $\Sigma = \mathbb{E}[\mathbf{s}\mathbf{s}'] \circ \mathbf{\Omega}$ .

Much of the literature focuses on the unstructured case where  $\mathbf{s}$  is a vector of independent, identically distributed elements and  $\mathbf{\Omega} \propto \mathbf{I}_p$ . This includes the Laplace prior, bridge/exponential power priors, normal-gamma priors, Dirichlet-Laplace priors, and horseshoe priors (Park and Casella, 2008; Griffin and Brown, 2010; Carvalho et al., 2010; Bhattacharya et al., 2015). These priors can be used to incorporate *a priori* knowledge of sparsity, by modeling a separate stochastic scale for every element of  $\beta$  and choosing distributions for  $\mathbf{s}$  that yield possibly sparse posterior modes. However, they do not allow elements of  $\beta$  to covary. Because the marginal covariance matrix  $\Sigma$  is an elementwise product of  $\mathbb{E}[\mathbf{s}\mathbf{s}']$  and  $\mathbf{\Omega}$ , elements of  $\beta$  are always uncorrelated *a priori* under these priors. The same limitation afflicts a new set of structured shrinkage priors, which model elements of  $\mathbf{s}$  as correlated but continue to assume that  $\mathbf{\Omega} \propto \mathbf{I}_p$  (van Gerven et al., 2010; Kalli and Griffin, 2014; Wu et al., 2014; Zhao et al., 2016; Kowal et al., 2017).

A different strand of literature models elements of  $\mathbf{s}$  as identical, with  $\mathbf{s} = s\mathbf{1}_p$ , and models elements of  $\mathbf{z}$  as correlated with a non-diagonal covariance matrix  $\mathbf{\Omega}$ . This includes all elliptically contoured prior distributions, and specifically the prior introduced by van Gerven et al. (2009). These priors can incorporate *a priori* knowledge of structure, as  $\Sigma \propto \mathbf{\Omega}$ . However, as these priors only have a single shrinkage factor  $s$ , they shrink all elements of  $\beta$  jointly and posterior modes based on these priors will only produce sparse estimates of

$\beta$  for which all entries are exactly equal to zero. Additionally, these priors do not generalize their independent counterparts. For instance, the multivariate Laplace prior with  $\Omega = \omega^2 \mathbf{I}_p$  does *not* correspond to the independent independent Laplace prior, and the corresponding penalty is the group lasso as opposed to the lasso penalty. While this may be appropriate in some settings, it will not be appropriate in settings where we are confident that only *some* elements of  $\beta$  are sparse, but unsure about the presence of structure.

At least one set of priors can incorporate *a priori* knowledge of structure and sparsity by additionally modeling elements of the inverse covariance matrix of  $\Omega$ . This includes the prior distribution that yields the fused lasso penalty  $\lambda_1 \|\beta\|_1 + \lambda_2 \sum_{i-j=1} |\beta_j - \beta_i|$  and priors that correspond to more general structured penalties of the form  $\beta' \mathbf{Q}^{-1} \beta + \lambda \|\beta\|_1$  where  $\mathbf{Q}^{-1}$  is positive semidefinite (Kyung et al., 2010; Ng and Abugharbieh, 2011; de Brecht and Yamagishi, 2012). These penalties corresponding to these priors are very popular, as they yield computationally feasible posterior mode optimization problems. Their main limitation is that relating the prior parameters  $\lambda_1$  and  $\lambda_2$  or  $\mathbf{Q}^{-1}$  and  $\lambda$  to the prior moments of  $\beta$  is prohibitively challenging. This makes it challenging for us to understand the exactly how flexible these priors are and makes specifying values or priors for these parameters difficult, as it is not possible to use moment-based empirical Bayes methods to set them and unclear how to relate the kind of *a priori* knowledge we might have to their values.

One last class of relevant priors are the structured normal-gamma priors introduced in Griffin and Brown (2012b) and Griffin and Brown (2012a), which are obtained by assuming  $\beta \stackrel{d}{=} \mathbf{C}(\mathbf{s} \circ \mathbf{z})$ , where  $\mathbf{C}$  is a  $p \times q$  rectangular matrix with  $p < q$  and  $s_j^2$  and  $z_j$  are independent gamma and normal random variables, respectively. Both elementwise and structured shrinkage can be simultaneously encouraged by setting  $\mathbf{C} = [\mathbf{I}_p, \mathbf{D}]$ , where  $\mathbf{D}$  is a  $p \times (q - p)$  matrix with columns that encode groups of elements of  $\beta$  that should be penalized jointly. However, the theory that justifies the use of these structured priors is specific to generalizing a single class of common sparsity inducing priors, specifically independent normal-gamma priors.

In this paper, we construct a class of “structured Hadamard product” (SHP) priors that can incorporate *a priori* knowledge of structure and sparsity by modeling elements of  $\mathbf{s}$  as independent and identically distributed, while allowing  $\Omega$ , and accordingly  $\Sigma$ ,

to be non-diagonal. The primary challenge in using such priors is computational. The marginal prior distributions for  $\beta$  are intractable integrals and correspond to penalties  $-\log(\int p(\beta|\Omega, \mathbf{s})d\mathbf{s})$  with no simple closed form, and require computationally demanding and non-standard Markov Chain Monte Carlo (MCMC) algorithms for posterior inference. As a result, the development of such priors has been largely ignored. An exception is Finegold and Drton (2011), which develops a multivariate  $t$ -distribution with nondiagonal  $\Omega$  by assuming that the squared scales  $s_j^2$  are independent and identically inverse-gamma distributed.

This paper proceeds as follows. In Section 2, we introduce three novel priors, the structured product normal (SPN), structured normal-gamma (SNG) and structured power/bridge (SPB) shrinkage prior distributions for penalized regression. The SPN and SNG priors generalize the normal-gamma priors described in Caron and Doucet (2008) and Griffin and Brown (2010), and the SPB priors generalize the power/bridge priors (Frank and Friedman, 1993; Polson et al., 2014). We discuss the properties of these priors in Section 3, specifically their behavior at the origin and along the axes, and the dependence structures they can accommodate. In Section 4, we describe how elliptical slice sampling can be used to overcome the computational issues that previously made posterior inference under such priors intractable, regardless of the distribution assumed for elements of  $\mathbf{s}$  (Murray et al., 2010), and discuss estimation of hyperparameters. For simplicity, we focus on problems where the log-likelihood of  $\beta$  can be written as conditionally quadratic in  $\beta$ , i.e.  $\exp\{-h(\mathbf{y}|\mathbf{X}, \beta)\} \propto_{\beta} \exp\{-\frac{1}{2}(\beta' \mathbf{A} \beta - 2\beta' \mathbf{c})\}$  for some positive definite matrix  $\mathbf{A}$  and real valued vector  $\mathbf{c}$ . This includes not only linear regression models but also certain latent variable representations of logistic and negative binomial regression models (Polson et al., 2013). In Section 5, we use several of our SHP priors to analyze the P300 speller data depicted in Figure 1. A discussion follows in Section 6.

## 2 Structured Shrinkage Priors

We define several “structured Hadamard product” (SHP) prior distributions for  $\beta$  of the form  $\beta = \mathbf{s} \circ \mathbf{z}$ , where ‘ $\circ$ ’ is the elementwise Hadamard product and  $\mathbf{z} \sim \text{normal}(\mathbf{0}, \Omega)$  and  $\mathbf{s}$  is a vector of stochastic scales that are independent of  $\mathbf{z}$ . Because the scales of elements

of  $\mathbf{s}$  are not separately identifiable from diagonal elements of  $\mathbf{\Omega}$ , we parametrize  $\mathbf{s}$  such that  $\mathbb{E}[s_j^2] = 1$  for  $j = 1, \dots, p$ . These priors are mean  $\mathbf{0}$  and have prior variance  $\mathbf{\Sigma} = \mathbb{E}[\mathbf{s}\mathbf{s}'] \circ \mathbf{\Omega}$ , but the marginal prior distributions  $p(\boldsymbol{\beta})$  are intractable integrals.

**Structured Product Normal (SPN) Prior:** When the stochastic scales  $\mathbf{s}$  are normally distributed,  $\mathbf{s} \sim \text{normal}(\mathbf{0}, \mathbf{\Psi})$ , and  $\mathbf{\Psi}$  is a non-diagonal, positive definite matrix with diagonal elements equal to 1, the structured product normal (SPN) prior is obtained. In this case, the parameters of the prior distribution for  $\mathbf{s}$ , denoted by  $\boldsymbol{\theta}$ , correspond to the off-diagonal elements of  $\mathbf{\Psi}$ . All of the elements of the hyperparameters  $\mathbf{\Omega}$  and  $\mathbf{\Psi}$  can be related to prior moments of  $\boldsymbol{\beta}$ . Diagonal elements of  $\mathbf{\Omega}$  correspond to prior variances of  $\boldsymbol{\beta}$ , and off diagonal elements of  $\mathbf{\Omega}$  and  $\mathbf{\Psi}$  determine covariances and fourth-order prior cross moments of  $\boldsymbol{\beta}$ , as shown in the appendix.

Originally discussed as a sparsity inducing penalty in Hoff (2017), the SPN prior is uniquely computationally simple to work with as the full conditional distributions of  $\mathbf{z}$  and  $\mathbf{s}$  are both multivariate normal distributions when the log-likelihood  $-h(\mathbf{y}|\mathbf{X}, \boldsymbol{\beta}, \boldsymbol{\phi})$  is quadratic or conditionally quadratic in  $\boldsymbol{\beta}$ . This is described in greater detail in Section 4. The SPN prior is also appealing as it is the only prior we define that has correlations among elements of  $\mathbf{s}$  and correlations among elements of  $\mathbf{z}$  *a priori*.

To reduce the number of freely varying parameters and to facilitate use of the SPN prior in settings where it is challenging to estimate or formulate prior opinions about fourth-order prior cross moments of  $\boldsymbol{\beta}$ , we also define a special case of the SPN prior which requires that the correlation matrix corresponding to  $\mathbf{\Omega}$  has elements that are equal in magnitude to the elements of  $\mathbf{\Psi}$ , i.e.  $|\omega_{ij}|/\sqrt{\omega_{ii}\omega_{jj}} = |\psi_{ij}|$ . We refer to this as the symmetric SPN (sSPN) prior. In this case, the prior distribution for  $\mathbf{s}$  has no prior parameters, i.e.  $\boldsymbol{\theta}$  is an empty vector for this class.

**Structured Normal-Gamma (SNG) Prior:** When the stochastic scales  $s_j^2$  are independent gamma random variables  $s_j^2 \sim \text{gamma}(c, c)$  with  $\mathbb{E}[s_j^2] = 1$  for fixed  $c \in (0, \infty)$ , the structured normal-gamma (SNG) prior is obtained. The SNG prior is a structured generalization of the normal-gamma prior of Griffin and Brown (2010). The shape parameter  $c$  is treated as a fixed value that parametrizes the prior class. As a result, the prior distribution

for  $\mathbf{s}$  has no prior parameters, i.e.  $\boldsymbol{\theta}$  is an empty vector for this class. The value chosen for  $c$  determines the prior fourth order moments of  $\boldsymbol{\beta}$ ; SNG priors with smaller values of  $c$  have lighter tails.

**Structured Power/Bridge (SPB) Prior:** When the stochastic scales  $s_j^2$  are independently distributed according to a polynomially tilted positive  $\alpha$ -stable distribution with index of stability  $\alpha = q/2$  and  $\mathbb{E}[s_j^2] = 1$  for fixed  $q \in (0, 2)$ , the structured power/bridge (SPB) prior is obtained. The SPB prior generalizes the bridge or exponential power prior discussed in Polson et al. (2014). The shape parameter  $q$  is treated as a fixed value that parametrizes the prior class. As a result, the prior distribution for  $\mathbf{s}$  has no prior parameters, i.e.  $\boldsymbol{\theta}$  is an empty vector for this class. Working with this prior is especially computationally challenging because the polynomially tilted positive  $\alpha$ -stable density  $p(s_j|\boldsymbol{\theta})$  is not available in closed form. Fortunately, a polynomially tilted positive  $\alpha$ -stable density that can be represented as a rate mixture of generalized gamma random variables (Devroye, 2009). This facilitates both simulating  $\boldsymbol{\beta}$  according to the SPB prior and simulating from the posterior distribution of  $\boldsymbol{\beta}$  under the SPB prior. A more detailed description of this representation and how it enables computation under the SPB prior is provided in the appendix. As with the SNG prior, the value chosen for  $q$  for the SPB prior determines the prior fourth order moments of  $\boldsymbol{\beta}$ ; SPB priors with larger values of  $q$  have lighter tails.

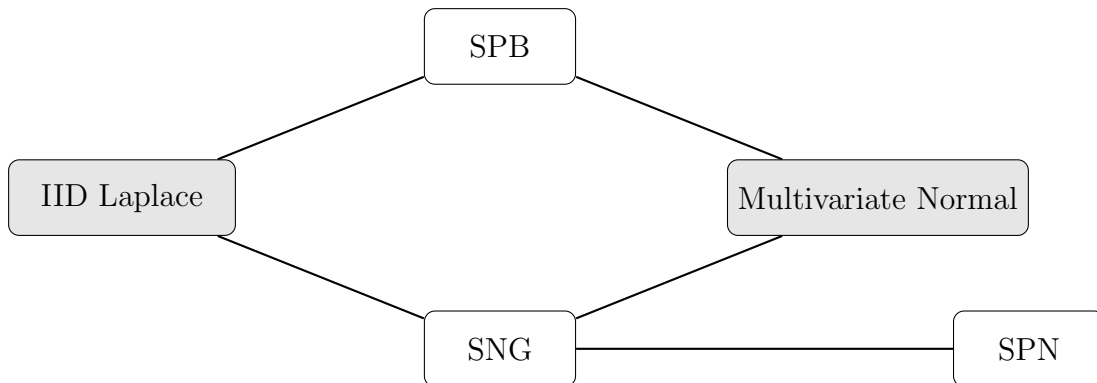


Figure 2: Relationships between structured product normal (SPN), structured normal-gamma (SNG) and structured power/bridge (SPB) shrinkage priors and independent, identically distributed (IID) Laplace and multivariate normal priors.



**Relationships Between SHP Priors:** Relationships between these priors, as well as the independent Laplace and multivariate normal distributions are depicted in Figure 2. The SNG and SPB priors are equivalent to each other when  $c = q = 1$  and they generalize the independent Laplace prior. Both the SNG and SPB priors also generalize the multivariate normal prior in the limit as  $c \rightarrow \infty$  or  $q \rightarrow 2$ . The SPN prior does not generalize the Laplace prior or the multivariate normal prior, but is equivalent to the SNG prior with  $c = 1/2$  when  $\Psi$  and  $\Omega$  are diagonal.

## 3 Properties

### 3.1 Univariate Prior Properties

In this section we explore properties of the induced marginal prior distributions of elements  $\beta_j$  under all three SHP priors on  $\beta$ . Importantly, introducing structure does not alter the marginal prior distributions of elements  $\beta_j$ . For instance, if we assume  $\beta$  has a structured prior that generalizes the independent Laplace prior, i.e.  $\beta$  has an SNG prior with  $c = 1$  or an SPB prior with  $q = 1$ , the marginal prior distribution of any element  $\beta_j$  is Laplace.

This is clear from the stochastic representation of elements  $\beta$  under these priors,  $\beta = \mathbf{s} \circ \mathbf{z}$ . Recall that  $\mathbf{s}$  is a vector of stochastic scales,  $\mathbf{z} \sim \text{normal}(\mathbf{0}, \Omega)$ ,  $\mathbf{s}$  and  $\mathbf{z}$  are independent of each other, and that all three SHP priors are obtained by assuming different distributions for  $\mathbf{s}$ . Under the SNG and SPB priors, structure is introduced by assuming  $\Omega$  is not diagonal, whereas under the SPN prior structure is introduced by assuming that  $\Omega$  is not diagonal and elements of  $\mathbf{s}$  have nondiagonal covariance  $\Psi$ . If we consider an individual element  $\beta_j = s_j z_j$  under the SNG or SPB priors, introducing structure does not affect  $s_j$  at all and does not affect the marginal distribution of  $z_j$ , as the marginal distribution of an element of a correlated normal vector is still normal. Similarly, if we consider an individual element  $\beta_j = s_j z_j$  under the SPN prior, introducing structure does not affect the marginal distributions of  $s_j$  and  $z_j$ , again because the marginal distribution of an element of a correlated normal vector is still normal.

Because introducing structure does not alter the marginal prior distributions of elements  $\beta_j$ , the marginal prior distributions of elements  $\beta_j$  retain the same sparsity inducing prop-

erties of the corresponding independent shrinkage priors. Specifically, The SNG and SPN priors generalize the entire class of independent normal-gamma priors and the independent normal-gamma prior with  $c = 1/2$ , respectively. Independent normal-gamma priors with  $c \leq 1/2$  are known to have an infinite spike or pole at  $b_j = 0$ , which has been viewed in the literature as a sufficient condition for the recovery of sparse signals (Carvalho et al., 2010; Griffin and Brown, 2010; Bhattacharya et al., 2015). Because introducing structure does not alter the marginal prior distributions of elements  $\beta_j$ , the marginal prior distributions of elements  $\beta_j$  under SNG priors with  $c \leq 1/2$  and under the SPN prior will also have an infinite spike or pole at  $b_j = 0$ . An additional proof of these results is given in the appendix.

## 3.2 Joint Prior Properties

### 3.2.1 Range of Achievable $\Sigma$

Although we have demonstrated that it is possible to construct structured or dependent generalizations of several independent shrinkage priors, introducing structure while retaining elementwise shrinkage can come at a cost. Specifically, under the SNG, SPB and SPN priors, preserving elementwise shrinkage limits how correlated elements of  $\beta$  can be.

Recall that under all three SHP priors, the prior covariance matrix of  $\beta$  is  $\Sigma = \mathbb{E}[\mathbf{s}\mathbf{s}'] \circ \Omega$ . Under the SNG and SPB priors,  $\mathbb{E}[\mathbf{s}\mathbf{s}']$  is constant for fixed values of  $c$  or  $q$ . Diagonal elements of  $\mathbb{E}[\mathbf{s}\mathbf{s}']$  are equal to 1, whereas off-diagonal elements are less than one in absolute value. Thus,  $\mathbb{E}[\mathbf{s}\mathbf{s}']$  shrinks off-diagonal elements of  $\Omega$ , reducing dependence. When  $\beta \in \mathbb{R}^2$ , we can explicitly calculate the maximum marginal prior correlation  $\rho$  under the SNG and SPB priors as a function of  $c$  or  $q$ . Under the SNG prior, the maximum correlation is equal to  $c^{-1}(\Gamma(c + 1/2)/\Gamma(c))^2$  and under the SPB prior, the maximum correlation is equal to  $(\pi/2)(\Gamma(2/q)/\sqrt{\Gamma(1/q)\Gamma(3/q)})^2$ . When  $q = c = 1$  and both priors are equivalent, the maximum correlation is equal to  $\pi/4 \approx 0.79$ .

We plot the maximum correlation as a function of kurtosis, a measure of tail behavior, under both priors in Figure 3. We observe greater reductions in the maximum correlation when the kurtosis is higher, and under the SNG prior relative to a SPB prior with equal kurtosis. The restricted range of  $\Sigma$  under the SNG and SPB priors is similar to the restricted range of the variance-covariance matrix of the alternative multivariate  $t$ -distribution intro-

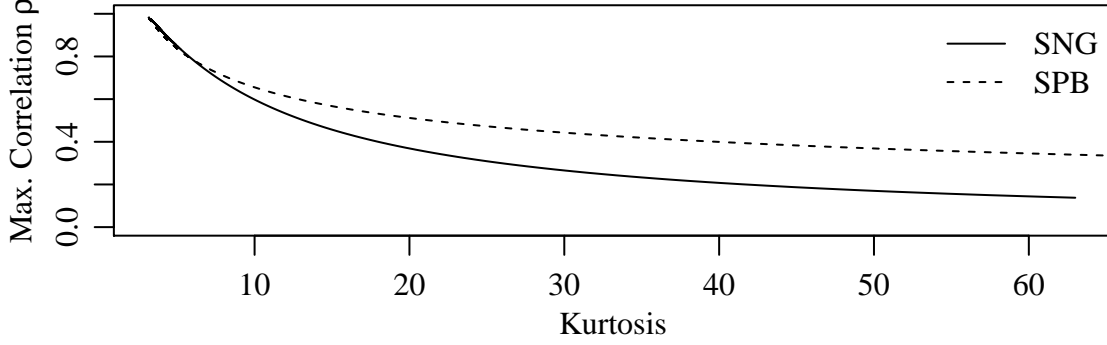


Figure 3: Maximum marginal prior correlation  $\rho$  for  $\beta \in \mathbb{R}^2$  as a function of kurtosis.

duced in Finegold and Drton (2011). Intuitively, the restricted range of  $\Sigma$  relates to the conflict that arises between the properties of the marginal joint density  $p(\beta|\Omega, \theta)$  needed to preserve elementwise shrinkage, specifically concentration of the density along the axes, and the properties of the marginal joint density needed to encourage structure, specifically concentration of the density along a line when  $p = 2$ .

In contrast, the unrestricted SPN prior can accommodate an arbitrary prior covariance  $\Sigma$ . Given a positive semidefinite prior covariance  $\Sigma$ , it is always possible to find at least one pair of positive semidefinite covariance matrices  $\Omega$  and  $\Psi$  that satisfy  $\Sigma = \Omega \circ \Psi$  (Styan, 1973). The sSPN prior is less flexible. It is easy to simulate a positive semidefinite covariance matrix  $\Sigma$  for which the corresponding values of  $\Omega$  or  $\Psi$  satisfying  $|\omega_{ij}| = |\psi_{ij}|$  are not positive semidefinite, but challenging to explicitly characterize the class of covariance matrices  $\Sigma$  that correspond to non-positive semidefinite values of  $\Omega$  or  $\Psi$ .

### 3.2.2 Copulas

Even when all three SHP priors share the same prior covariance matrix  $\Sigma$ , the induced dependence structures vary widely. We compare the induced dependence structures by considering  $\beta \in \mathbb{R}^2$  with unit marginal variances and correlation  $\rho = 0.5$ , and examining corresponding copula densities. Let  $F_j^{SNG,1}(\beta_j)$  refer to the marginal prior CDF of  $\beta_j$  corresponding to one of the SHP prior distributions, we can always write  $\beta_j \stackrel{d}{=} F_j^{-1}(u_j)$ , where  $u_j$  is a random variable with uniform margins. The joint distribution of the  $p \times 1$  vector  $\mathbf{u}$  is called the copula of  $\beta$ , and it characterizes the induced dependence structure.

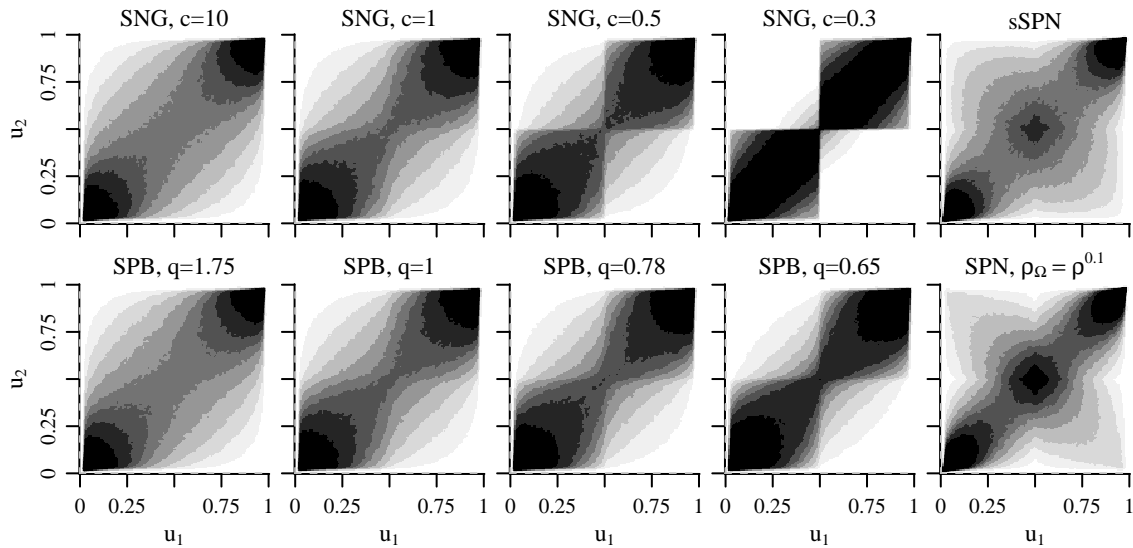


Figure 4: Approximate copula densities for  $\beta \in \mathbb{R}^2$  with unit marginal prior variances and marginal prior correlation  $\rho = 0.5$ . Copula density approximations were made by simulating 1,000,000 values from the corresponding prior, transforming simulated values of  $\beta_1$  and  $\beta_2$  into percentiles  $u_1$  and  $u_2$ , and computing a kernel bivariate density estimate of the percentiles.

Even if the inverse CDF's  $F_j^{-1}(u_j)$  are not known, the copula density can be approximated by simulating values of  $\beta$ , transforming simulated values of  $\beta_1$  and  $\beta_2$  into percentiles  $u_1$  and  $u_2$ , and computing a kernel bivariate density estimate of the percentiles. Figure 4 shows numerical approximations to copula densities for several cases of all three SHP priors with unit marginal prior variances and marginal prior correlation  $\rho = 0.5$ .

The first four panels in the top and bottom rows show copula densities under SNG and SPB priors with increasingly heavy tails, and the final panels on the top and bottom show conditional prior distributions under SPN priors with  $\rho_{\Omega} = \rho^{0.5}$  and  $\rho_{\Omega} = \rho^{0.1}$ . The parameters of the SPB priors have been chosen to ensure that the kurtosis, a measure of tail behavior, of each SPB prior is equal to the kurtosis of the SNG prior above it, e.g. the SNG prior with  $c = 0.3$  has the same kurtosis as the SPB prior with  $q = 0.65$ .

The dependance structures induced by the SNG and SPB priors are similar. As  $c$  or  $q \rightarrow 0$  and the SNG and SPB priors become less normal and heavier tailed, the copulas display increasingly strong orthant dependence. This means that as  $c$  or  $q \rightarrow 0$ , the

priors concentrate more strongly around values of  $\beta$  that have the same sign. The SNG prior displays especially strong orthant dependence and appears to converge to a uniform distribution over the positive and negative orthants as  $c \rightarrow 0$ . Additionally, as  $c$  or  $q \rightarrow 0$  the copula densities become more concentrated around the axes where at least one element of  $\beta$  is nearly or exactly equal to zero, suggesting that these priors are still encouraging elementwise shrinkage.

Like the SNG and SPB priors, the SPN priors concentrate in the upper-right and lower-left corners, where  $\beta_1$  and  $\beta_2$  have the same sign and are large in magnitude. However in comparison to the SNG and SPB priors, both SPN priors also concentrate strongly at the origin, where  $\beta_1 = \beta_2 = 0$ , and less strongly along the axes, where  $\beta_1 = 0$  or  $\beta_2 = 0$ . Both SPN priors also concentrate more about values of  $\beta$  that are similar in magnitude and opposite in sign. The extent of this depends on how  $\rho_\Omega$  is chosen. Compared to the sSPN prior which sets  $\rho_\Omega$  and  $\rho_\Psi$  symmetrically such that  $\rho_\Omega = \rho_\Psi$ , the SPN prior with  $\rho_\Omega = \rho^{0.1}$  and  $\rho_\Psi = \rho^{0.9}$  concentrates more strongly about values of  $\beta$  that are equal in magnitude but opposite in sign. Intuitively, this is due to the fact that  $\beta$  is made up of one strongly correlated component and one very weakly correlated component, both of which can take any value on  $\mathbb{R}$  when  $\rho_\Omega = \rho^{0.1}$  and  $\rho_\Psi = \rho^{0.9}$ .

### 3.2.3 Conditional Prior Distributions

We can explore how introducing structure can inform shrinkage of elements of  $\beta$  by examining the induced conditional prior distributions. Figure 5 shows conditional prior distributions  $p(\beta_1|\beta_2|\Omega, \theta)$ , for  $\beta \in \mathbb{R}^2$  with unit marginal prior variance, marginal prior correlations  $\rho = \{0, 0.5\}$ , and  $\beta_2 = \{0, 2\}$ . Again, the first four panels in the top and bottom rows show conditional prior distributions under SNG and SPB priors with increasingly heavy tails, and the final panels on the top and bottom show conditional prior distributions under SPN priors with  $\rho_\Omega = \rho^{0.5}$  and  $\rho_\Omega = \rho^{0.1}$ . The parameters of the SPB priors have been chosen to ensure that the kurtosis, a measure of tail behavior, of each SPB prior is equal to the kurtosis of the SNG prior above it, e.g. the SNG prior with  $c = 0.3$  has the same kurtosis as the SPB prior with  $q = 0.65$ .

Introducing structure via a positive prior correlation between  $\beta_1$  and  $\beta_2$  can allow us

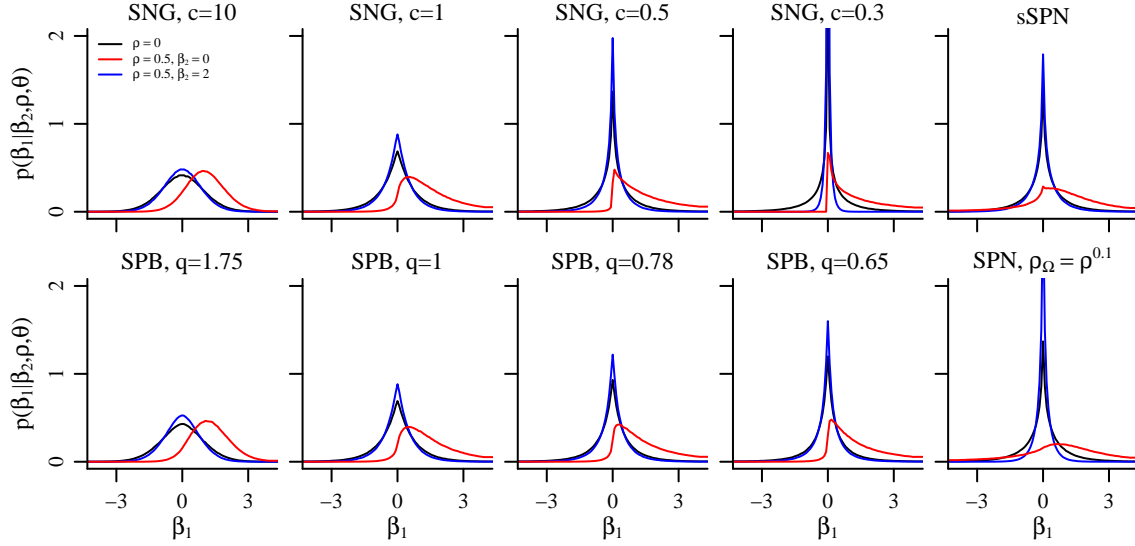


Figure 5: Conditional prior distributions  $p(\beta_1|\beta_2, \rho, \theta)$  for  $\beta \in \mathbb{R}^2$  with unit marginal prior variances, marginal prior correlation  $\rho \in \{0, 0.5\}$  and  $\beta_2 \in \{0, 2\}$  obtained via simulation.

to use knowledge of  $\beta_2$  to better estimate  $\beta_1$ . We see that sparsity inducing SHP priors concentrate more strongly about zero than their independent counterparts when  $\beta_2 = 0$ , and shift their mass towards positive nonzero values of  $\beta_1$  when  $\beta_2 = 2$ . The conditional priors reflect differing amounts of origin versus tail dependence. The nearly normal SNG and SPB priors on the far left display relatively more tail dependence, as the structured conditional priors for  $\beta_1$  differ more from their independent counterparts when  $\beta_2 = 2$  than when  $\beta_2 = 0$ . At the other end of the spectrum, the heavier-than-Laplace tailed SNG and SPB priors and the sSPN prior display more origin dependence than tail dependence, as the structured conditional priors for  $\beta_1$  concentrate much more strongly about  $\beta_1 = 0$  when  $\beta_2 = 0$  than their independent counterparts, and still have a near  $\beta_1 = 0$  even when  $\beta_2 = 2$ . This is especially striking under the SNG priors with  $c \leq 1/2$  and the sSPN prior, which retain a very sharp peak at  $\beta_1 = 0$  even when  $\beta_2 = 2$ . Interesting, the asymmetric SPN prior with  $\rho_\Omega = \rho^{0.1}$  is in between; the full conditional distribution of  $\beta_1$  concentrates much more strongly about  $\beta_1 = 0$  when  $\beta_2 = 0$  and shifts markedly to towards  $\beta_1 = 2$  when  $\beta_2 = 2$ .

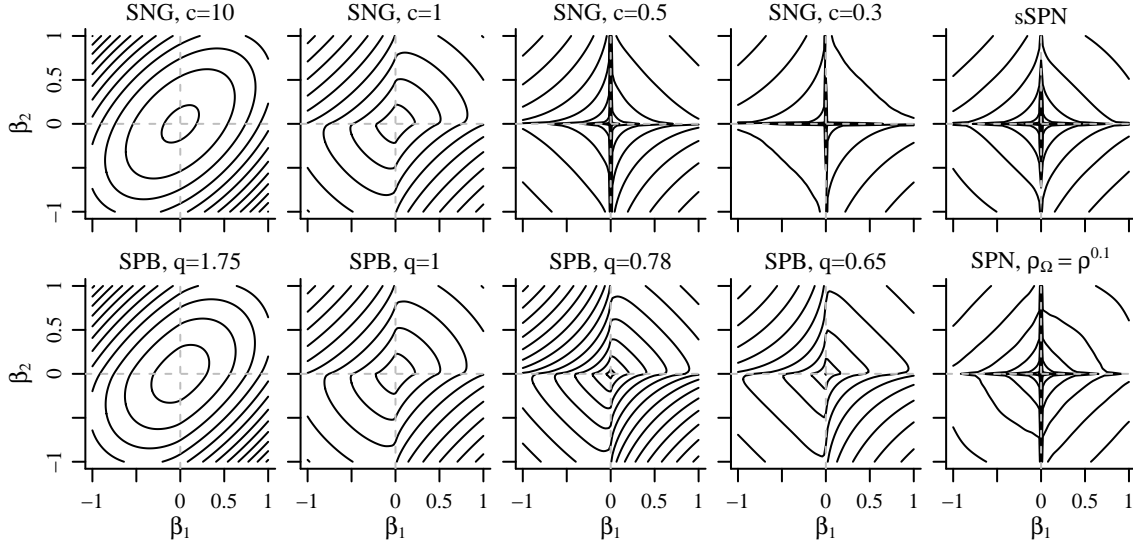


Figure 6: Prior density contours for  $\beta \in \mathbb{R}^2$  with unit marginal prior variance and marginal prior correlation  $\rho = 0.5$ .

### 3.2.4 Joint Marginal Prior Contours

The joint marginal prior contours, which can be interpreted as contours of a penalty function, provide a powerful tool for studying the properties of different priors. Figure 6 shows Monte Carlo approximations of the contours of the joint marginal priors  $\int p(\beta|\mathbf{s}, \Omega)p(\mathbf{s}|\boldsymbol{\theta})d\mathbf{s}$ , for  $\beta \in \mathbb{R}^2$  with marginal prior variance-covariance matrix  $\Sigma = (1 - \rho)\mathbf{I}_2 + \rho\mathbf{1}_2\mathbf{1}_2'$  and marginal prior correlation  $\rho = 0.5$ .

Again, the first four panels in the top and bottom rows show contours of SNG and SPB priors with increasingly heavy tails. The parameters of the SPB priors have been chosen to ensure that the kurtosis, a measure of tail behavior, of each SPB prior is equal to the kurtosis of the SNG prior above it, e.g. the SNG prior with  $c = 0.3$  has the same kurtosis as the SPB prior with  $q = 0.65$ . The rightmost panels show contours of SPN priors. The top panel is a symmetric sSPN prior with  $\rho_\Omega = \rho^{0.5}$  and  $\rho_\Psi = \rho^{0.5}$ , whereas the bottom panel is an asymmetric SPN prior with  $\rho_\Omega = \rho^{0.1}$  and  $\rho_\Psi = \rho^{0.9}$ .

All three SHP priors encourage similar estimates of  $\beta_1$  and  $\beta_2$  by pushing contours away from the origin when  $\beta_1$  and  $\beta_2$  have the same sign and pushing the contours towards the origin when  $\beta_1$  and  $\beta_2$  have opposite signs. The SPN, SNG with  $c \leq 1$  and SPB with

$q \leq 1$  priors encourage sparse estimates of  $\beta$  by retaining discontinuities of the log marginal prior on the axes. Interestingly, the contours do not necessarily keep the same shape as the value of prior density changes. Contours closer to the origin are more similar to their independent counterparts, with relatively more encouragement of sparsity than structure, whereas contours farther from the origin tend to encourage relatively more structure and less sparsity. This is especially evident under the SPN prior with  $\rho_\omega = \rho^{0.1}$ . We note that it is clear from the contours that these priors are *not* log-concave when  $\rho \neq 0$  and accordingly correspond to *non-convex* penalties under SNG priors with  $c \leq 1$ , the SPB priors with  $q \leq 1$ , and the SPN and sSPN priors.

Under the SNG priors with  $c \leq 1/2$  and the SPN priors, we see that the contours do not cross the axes. This is a consequence of the behavior of these joint priors along the axes. The joint marginal distribution of  $\beta$  under the SNG prior with  $c \leq 1/2$  has an infinite spike or pole along the axes, when at least one element of  $\mathbf{b}$  is equal to 0.

**Proposition 3.1** *For the SNG prior, if  $c < 1/2$  and  $b_j = 0$  for any  $j \in \{1, \dots, p\}$ , then  $p(\mathbf{b}|c, \Omega) = +\infty$ .*

This is a multivariate analogue of the univariate marginal prior’s spike or infinite pole at  $b = 0$  under the SNG prior with  $c \leq 1/2$ . The joint marginal SPN prior behaves similarly along the axes.

**Proposition 3.2** *For the SPN prior, if  $b_j = 0$  for any  $j \in \{1, \dots, p\}$ , then  $p(\mathbf{b}|\Psi, \Omega) = +\infty$ .*

Proofs of these propositions are given in the appendix. This suggests that the SPN and SNG priors with  $c < 1/2$  may recover sparse signals well (Carvalho et al., 2010; Griffin and Brown, 2010; Bhattacharya et al., 2015). However the presence of an infinite spike or pole at  $b_j = 0$  also makes the already challenging problem of computing the posterior mode intractable, as the log marginal prior is not only nonconvex but also has infinitely many modes.



### 3.3 Posterior Properties

One last perspective on the properties of all three SHP priors can be gained by examining how the posterior mode of  $\beta$  relates to the unpenalized OLS estimate  $\hat{\beta}_{OLS}$ . This can offer an intuitive understanding of the properties of estimators obtained under the three different priors. In the sparsity inducing penalty literature this is often characterized by the thresholding function, which is defined in the context of linear model for  $\mathbf{y}$  with a single covariate  $\mathbf{x}$  that satisfies  $\mathbf{x}'\mathbf{x} = 1$  as

$$\hat{\beta} = \operatorname{argmin}_{\beta} \frac{1}{2\phi^2} \left( \hat{\beta}_{OLS} - \beta \right)^2 + \log \left( \int p(\beta|s, \omega) p(s|\theta) ds \right). \quad (1)$$

For example, (1) gives the soft-thresholding function when  $\beta$  has a mean-zero Laplace distribution.

Because the advantage of working with any of the three SHP priors is the ability to introduce a priori dependence across elements of vector valued  $\beta$ , examining the corresponding univariate thresholding functions for scalar  $\beta$  given by (1) does not fully explore how the posterior mode of  $\beta$  relates to the unpenalized OLS estimate  $\hat{\beta}$ . Accordingly, we define and examine a bivariate thresholding function. We continue to assume a linear model for  $\mathbf{y}$ , but assume an orthogonal design matrix comprised of two covariates  $\mathbf{X}$  that satisfies  $\mathbf{X}'\mathbf{X} = \operatorname{diag}\{\mathbf{1}_2\}$  instead of a single covariate  $\mathbf{x}$ . The bivariate thresholding function relates the posterior mode of both  $\beta_1$  and  $\beta_2$  to the noise variance  $\phi^2$ , prior parameters  $\Omega$  and  $\theta$ , and OLS estimates  $\hat{\beta}_{OLS,1}$  and  $\hat{\beta}_{OLS,2}$ , and is given by

$$\hat{\beta} = \operatorname{argmin}_{\beta} \frac{1}{2\phi^2} \left\| \hat{\beta}_{OLS} - \beta \right\|_2^2 + \log \left( \int p(\beta|\mathbf{s}, \Omega) p(\mathbf{s}|\theta) d\mathbf{s} \right). \quad (2)$$

Although it is not available in closed form, the bivariate thresholding function can be approximated using a Gibbs-within-EM algorithm described in the Section 4. Figure 7 shows approximate bivariate thresholding functions for  $\beta \in \mathbb{R}^2$  with unit marginal prior variances, marginal prior correlation  $\rho = 0.5$ , noise variance  $\phi^2 = 0.1$ ,  $\hat{\beta}_{OLS,2} \in \{-0.5, 0, 0.5, 1\}$  and  $\hat{\beta}_{OLS,1} \in [0, 1]$ , computed from 1,001,000 Gibbs sampler iterations, with the first 1,000 samples discarded as burn-in.

Examination of the bivariate thresholding functions confirms that the SPN prior, SNG prior with  $c \leq 1$  and SPB prior with  $c \leq 1$  can yield possibly sparse posterior mode

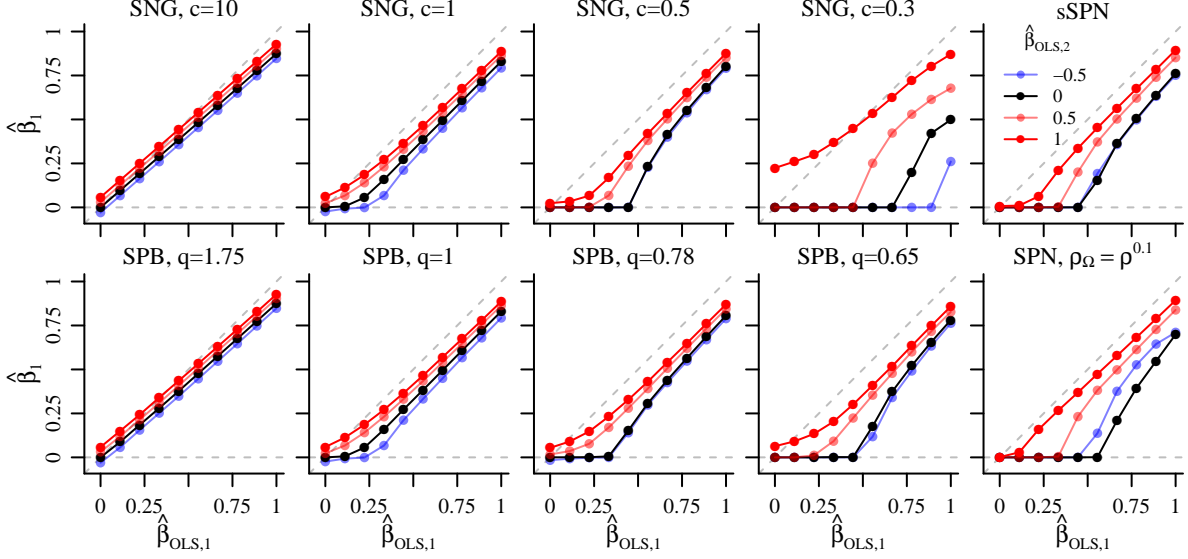


Figure 7: Approximate bivariate thresholding functions computed according to (2) for  $\beta \in \mathbb{R}^2$  with unit marginal prior variances, marginal prior correlation  $\rho = 0.5$ , noise variance  $\phi^2 = 0.1$ ,  $\hat{\beta}_{OLS,2} \in \{-0.5, 0, 0.5, 1\}$  and  $\hat{\beta}_{OLS,1} \in (0, 1)$ .

estimates of  $\beta$ , and that the introduction of structure encourages or discourages sparse estimates  $\hat{\beta}_1$  depending not only on the observed value of  $\hat{\beta}_{OLS,1}$  but also the observed value of  $\hat{\beta}_{OLS,2}$ .

There are a few interesting trends that relate to previously identified properties of the SPN, SNG and SPB priors. We observe that both SPN priors shrink  $\hat{\beta}_1$  towards 0 more aggressively when  $\hat{\beta}_{OLS,2} = -0.5$  than when  $\hat{\beta}_{OLS,2} = 0$ , which reflects the tendency of the SPN priors to encourage not only estimates of  $\beta$  with similar signs but also similar magnitudes. Additionally, the value of  $\hat{\beta}_{OLS,2}$  appears to affect the estimate  $\hat{\beta}_1$  more when  $\hat{\beta}_{OLS,1}$  is smaller under the SPN prior, SNG prior with  $c \leq 1$  and SPB prior with  $c \leq 1$ . This is consistent with what we observed when examining the copulas and conditional prior distributions; as the tails become heavier, the Laplace and heavier-than Laplace prior distributions display more dependence at the origin than the tails. Last, we observe that the SNG prior with  $c = 0.3$  not only induces especially strong shrinkage of  $\hat{\beta}_1$  when  $\hat{\beta}_{OLS,2}$  is small, but also induces aggressive inflation of  $\hat{\beta}_1$  when  $\hat{\beta}_{OLS,1}$  is small and  $\hat{\beta}_{OLS,2}$  is very large. This makes sense in the context of the prior conditional distributions under the SNG and SPB priors with  $c = 0.3$  and  $q = 0.65$ . Although these two priors have equally heavy

tails, the SNG prior is much more concentrated at the origin and has heavier tails.

## 4 Computation

### 4.1 Posterior Approximation

The posterior mode of  $\beta$  maximizes the integral  $\int p(\mathbf{y}|\mathbf{X}, \beta, \phi) p(\beta|\Omega, \mathbf{s}) p(\mathbf{s}|\theta) d\mathbf{s}$  over  $\beta$ . As noted previously, we can also think of the posterior mode as a penalized estimate of  $\beta$ , where the penalty is given by  $-\log(\int p(\beta|\Omega, \mathbf{s}) p(\mathbf{s}|\theta) d\mathbf{s})$ . This integral is generally intractable when  $\Omega$  is not diagonal, but can be maximized using an MCMC within Expectation Maximization (EM) algorithm (Dempster et al., 1977). Given an initial value  $\beta^{(0)}$ , this algorithm proceeds by iterating the following until  $\|\beta^{(i+1)} - \beta^{(i)}\|_2^2$  converges:

- using MCMC to simulate  $M$  draws  $\mathbf{s}^{(1)}, \dots, \mathbf{s}^{(M)}$  from the full conditional distribution of  $\mathbf{s}$  given  $\beta^{(i)}$  and  $\theta$ , set  $\widehat{\mathbb{E}}[(\frac{1}{\mathbf{s}})(\frac{1}{\mathbf{s}})'|\beta^{(i)}, \theta] = \frac{1}{M} \sum_{j=1}^M (\frac{1}{\mathbf{s}^{(j)}})(\frac{1}{\mathbf{s}^{(j)}})'$ ;
- set  $\beta^{(i+1)} = \operatorname{argmin}_{\beta} h(\mathbf{y}|\mathbf{X}, \beta, \phi) + \frac{1}{2} \beta' (\Omega^{-1} \circ \widehat{\mathbb{E}}[(\frac{1}{\mathbf{s}})(\frac{1}{\mathbf{s}})'|\beta^{(i)}, \theta]) \beta$ .

Alternative posterior summaries can be obtained by simulating  $M$  values  $\beta^{(1)}, \dots, \beta^{(M)}$  from the joint posterior distribution of  $(\beta, \mathbf{s})$  given  $\mathbf{y}$ ,  $\mathbf{X}$ ,  $\phi$  and  $\theta$  given an initial value  $\beta^{(0)}$  by iteratively simulating  $\mathbf{s}^{(j)}$  from the full conditional distribution of  $\mathbf{s}$  given  $\beta^{(j-1)}$  and  $\theta$  and simulating  $\beta^{(j)}$  from the full conditional distribution of  $\beta$  given  $\mathbf{y}$ ,  $\mathbf{X}$ ,  $\mathbf{s}^{(j)}$  and  $\phi$ . The posterior mean of  $\beta$  can be obtained by computing the sample mean  $\frac{1}{M} \sum_{j=1}^M \beta^{(j)}$ , and alternative posterior summaries can be obtained by computing the corresponding sample quantities for  $\beta^{(1)}, \dots, \beta^{(M)}$ . When the log-likelihood is quadratic or conditionally quadratic in  $\beta$ , the full conditional distribution  $p(\beta|\mathbf{s}, \mathbf{y}, \mathbf{X}, \phi)$  is a multivariate normal distribution and accordingly straightforward to simulate from.

Given any prior  $p(\mathbf{s}|\theta)$ , the full conditional distribution  $p(\mathbf{s}|\beta, \Omega, \theta)$  can be written as proportional to

$$\left( \prod_{j=1}^p |s_j|^{-1} \right) \exp \left\{ -\frac{1}{2} (\mathbf{1}/\mathbf{s})' (\Omega^{-1} \circ (\beta\beta')) (\mathbf{1}/\mathbf{s}) \right\} p(\mathbf{s}|\theta), \quad (3)$$

where ‘/’ is applied elementwise. The choices  $p(\mathbf{s}|\boldsymbol{\theta})$  that yield the SPN, SNG and SPB models do not yield standard distributions when  $\boldsymbol{\Omega}$  is not a diagonal matrix.

We simulate from the full conditional distribution (3) using an approach related to generalized elliptical slice sampling (Nishihara et al., 2014). Simulating  $\mathbf{s}$  according to (3) is equivalent to simulating  $\mathbf{r}$ ,  $\mathbf{u}$ ,  $\mathbf{w}$  and  $\boldsymbol{\pi}$  according to

$$\left( \prod_{j=1}^p \int_0^\infty w_j^{\frac{\nu+1}{2}-1} \exp \left\{ -w_j \left( \frac{\nu}{2} + \frac{r_j^2 + u_j^2}{2v_j^2} \right) \right\} dw_j \right) \left( \frac{p(\mathbf{s}|\boldsymbol{\beta}, \boldsymbol{\Omega}, \boldsymbol{\theta})}{\left( \prod_{j=1}^p \left( 1 + \frac{(s_j - m_j)^2}{v_j^2 \nu} \right)^{-\frac{\nu+1}{2}} \right)} \right), \quad (4)$$

where  $\mathbf{s} = \mathbf{u}\sin(\boldsymbol{\pi}) + \mathbf{r}\cos(\boldsymbol{\pi}) + \mathbf{m}$  under the SPN prior and  $\mathbf{s} = |\mathbf{u}\sin(\boldsymbol{\pi}) + \mathbf{r}\cos(\boldsymbol{\pi}) + \mathbf{m}|$  under the SNG or SPB priors and  $\mathbf{m}$  and  $\mathbf{v}$  are fixed and known location and scale parameters and  $\nu$  is a fixed and known degrees of freedom.

For fixed  $\mathbf{m}$ ,  $\mathbf{v}$ , and  $\nu$ , iteration  $i$  of a Gibbs sampler simulating from (4) is as follows:

1. Simulate  $w_j^{(i)} \sim \text{gamma}(\frac{\nu+1}{2}, \frac{\nu}{2} + \frac{(r_j^{(i-1)} - m_j)^2 + (u_j^{(i-1)} - m_j)^2}{2(v_j^2)^{(i-1)}})$  for  $j = 1, \dots, p$ .
2. Simulate  $t_j^{(i)} \sim \text{normal}(0, \frac{v_j^2}{w_j^{(i)}})$  for  $j = 1, \dots, p$ .
3. Set  $\mathbf{u}^{(i)} = (\mathbf{s}^{(i-1)} - \mathbf{m})\sin(\boldsymbol{\pi}^{(i-1)}) + \mathbf{t}^{(i)}\cos(\boldsymbol{\pi}^{(i-1)})$ .
4. Set  $\mathbf{r}^{(i)} = (\mathbf{s}^{(i-1)} - \mathbf{m})\cos(\boldsymbol{\pi}^{(i-1)}) - \mathbf{t}^{(i)}\sin(\boldsymbol{\pi}^{(i-1)})$ .
5. Simulate unique elements of  $\boldsymbol{\pi}$  according to (4) individually using univariate slice sampling as described in the appendix.
6. Set  $\mathbf{s}^{(i)} = \mathbf{u}^{(i)}\sin(\boldsymbol{\pi}^{(i)}) + \mathbf{r}^{(i)}\cos(\boldsymbol{\pi}^{(i)}) + \mathbf{m}$  if using the SPN prior.  
Set  $\mathbf{s}^{(i)} = |\mathbf{u}^{(i)}\sin(\boldsymbol{\pi}^{(i)}) + \mathbf{r}^{(i)}\cos(\boldsymbol{\pi}^{(i)}) + \mathbf{m}|$  if using the SNG or SPB prior.

We can think of steps 1-4 as generating a proposal for  $\mathbf{s}^{(i)}$  and step 5 as generating an adjustment for the proposal that reflects the relationship between the proposal distribution and the target full conditional distribution. The locations  $\mathbf{m}$ , scales  $\mathbf{v}$ , degrees of freedom  $\nu$ , and number of unique slice variables contained in  $\boldsymbol{\pi}$  can be chosen to improve sampling and decrease computational burden. Choices of  $\mathbf{m}$ ,  $\mathbf{v}$  and  $\eta$  that provide better approximations to the full conditional distribution  $p(\mathbf{s}|\boldsymbol{\beta}, \boldsymbol{\Omega}, \boldsymbol{\theta})$  are likely to result in better mixing, whereas

choices of  $\mathbf{m}$  and  $\mathbf{v}$  that are easier to compute will improve the speed of the sampling process.

We suggest choosing  $\mathbf{m}$  to be an approximate mode of  $p(\mathbf{s}|\boldsymbol{\beta}, \boldsymbol{\Omega}, \boldsymbol{\theta})$ , obtained by performing coordinate descent with a large convergence threshold and a small number of maximum iterations of coordinate descent. We describe how  $\mathbf{m}$  can be obtained quickly via coordinate descent under any of the SHP priors in the appendix. Letting  $f_j(\mathbf{s}, \boldsymbol{\beta}, \boldsymbol{\Omega}, \boldsymbol{\theta}) = \frac{\partial}{\partial s_j^2} p(\mathbf{s}|\boldsymbol{\beta}, \boldsymbol{\Omega}, \boldsymbol{\theta})$ , we suggest setting  $\mathbf{v} = \mathbf{1}/\sqrt{-\mathbf{f}(\tilde{\mathbf{m}}, \boldsymbol{\beta}, \boldsymbol{\Omega}, \boldsymbol{\theta})}$ , where  $\tilde{m}_j = m_j$  if  $|m_j| > 10^{-12}$  and  $\tilde{m}_j = \text{sign}(m_j) \times 10^{-12}$  otherwise, which roughly approximates the variance of  $p(\mathbf{s}|\boldsymbol{\beta}, \boldsymbol{\Omega}, \boldsymbol{\theta})$  about  $\mathbf{m}$ . Regarding  $\nu$ , it is important to choose a value large enough to ensure that the tails of the  $t$ -distributions are heavier than the tails of  $p(\mathbf{s}|\boldsymbol{\beta}, \boldsymbol{\Omega}, \boldsymbol{\theta})$ . We find that  $\nu = 1$  performs well in the situations we consider. Last, allowing all  $p$  elements of  $\boldsymbol{\pi}$  to be unique may yield a very slow sampling procedure as  $p$  additional values must be simulated during each iteration of the Gibbs sampler and simulating unique elements of  $\boldsymbol{\pi}$  as described cannot be generally be performed in parallel. At the same time, setting  $\boldsymbol{\pi} = \pi \mathbf{1}$  may yield a Gibbs sampler that mixes very slowly. We suggest partitioning  $\boldsymbol{\pi}$  into  $k$  unique elements that correspond to mutually exclusive groups of elements of  $\mathbf{s}$  that are expected to be correlated in the posterior distribution, as suggested by the structure of the design matrix  $\mathbf{X}$ . This partitioning procedure is described in greater detail in the appendix.

#### 4.1.1 Simulating from the Posterior Distribution under the SPN Prior

As noted in Section 2, it is uniquely simple to simulate from the joint posterior distribution under the SPN prior. In the linear regression setting with known unit variance where  $-h(\mathbf{y}|\mathbf{X}, \boldsymbol{\beta}) \propto_{\boldsymbol{\beta}} \frac{1}{2}(\boldsymbol{\beta}' \mathbf{X}' \mathbf{X} \boldsymbol{\beta} - 2\boldsymbol{\beta}' \mathbf{X}' \mathbf{y})$ , then

$$\begin{aligned} \mathbf{z}|\mathbf{X}, \mathbf{y}, \mathbf{s}, \boldsymbol{\Omega} &\sim \text{normal} \left( ((\mathbf{X}' \mathbf{X}) \circ (\mathbf{s} \mathbf{s}') + \boldsymbol{\Omega}^{-1})^{-1} (\mathbf{s} \circ (\mathbf{X}' \mathbf{y})), ((\mathbf{X}' \mathbf{X}) \circ (\mathbf{s} \mathbf{s}') + \boldsymbol{\Omega}^{-1})^{-1} \right), \\ \mathbf{s}|\mathbf{X}, \mathbf{y}, \mathbf{z}, \boldsymbol{\Psi} &\sim \text{normal} \left( ((\mathbf{X}' \mathbf{X}) \circ (\mathbf{z} \mathbf{z}') + \boldsymbol{\Psi}^{-1})^{-1} (\mathbf{z} \circ (\mathbf{X}' \mathbf{y})), ((\mathbf{X}' \mathbf{X}) \circ (\mathbf{z} \mathbf{z}') + \boldsymbol{\Psi}^{-1})^{-1} \right). \end{aligned}$$

Both full conditional distributions are multivariate normal distributions. As a result, a straightforward Gibbs sampler using standard distributions can be used to simulate from the joint posterior distribution.

## 4.2 Hyperparameter Estimation

In the previous subsection, we presented a general approach for simulating from the posterior distribution of  $\beta$  under the SPN, SNG and SPB priors given hyperparameters  $\Omega$  and, in the case of the SPN prior,  $\Psi$ . One simple approach to estimating these hyperparameters is to perform fully Bayes inference, assuming prior distributions for  $\phi$ ,  $\Omega$ , and/or  $\Psi$ . For all three priors, a conjugate inverse-Wishart prior for  $\Omega$  is a natural choice. For the SPN prior, a conjugate inverse-Wishart prior for  $\Psi$  is likewise natural. However, using a fully Bayesian approach will no longer produce a possibly sparse posterior mode.

If a possible sparse posterior mode estimate is desired, hyperparameter estimates can be obtained via maximum marginal likelihood estimation (MMLE) or the method of moments. Alternatively, we can perform maximum marginal likelihood estimation (MMLE) of the unknown variance components  $\Omega$  and, in the case of the SPN prior,  $\Psi$ , using an Gibbs-within-EM algorithm as described in the appendix. However, maximum marginal likelihood estimation of hyperparameters can converge prohibitively slowly in practice (Roy and Chakraborty, 2016). Furthermore, the Gibbs step can be prohibitively computationally demanding when the data are high dimensional. Fortunately, method of moments type estimates of the unknown variance components can be obtained under the SNG and SPB priors for fixed  $c$  and  $q$  respectively, and under the symmetric sSPN prior, so long as  $y$  is linearly related to  $X\beta$ . As noted in the Introduction, the prior moments are easy to compute under all three priors

$$\mathbb{E}[\beta] = \mathbb{E}[s] \circ \mathbb{E}[z] \text{ and } \Sigma = \mathbb{E}[ss'] \circ \mathbb{E}[zz'].$$

Furthermore, under the sSPN, SNG and SPB priors, the hyperparameters are correspond to second order moments of  $\beta$ . When  $y$  is linearly related to  $X\beta$ , a positive semidefinite estimate of  $\Sigma$  can be obtained using methods from Perry (2017). Under the sSPN prior, estimates of  $\Omega$  and  $\Psi$  can be obtained from an estimate  $\hat{\Sigma}$  by projecting  $\sqrt{|\hat{\Sigma}|}$  and  $\text{sign}\{\hat{\Sigma}\}\sqrt{|\hat{\Sigma}|}$  onto the positive semi-definite cone, where  $\sqrt{\cdot}$ ,  $|\cdot|$  and  $\text{sign}\{\cdot\}$  are applied elementwise. Under the SNG and SPB priors, an estimate of  $\Omega$  can be obtained from an estimate  $\hat{\Sigma}$  by projecting  $\hat{\Sigma}/((1 - \mathbb{E}[s_j]^2)\mathbf{I}_p + \mathbb{E}[s_j]^2\mathbf{1}_p\mathbf{1}_p')$  onto the positive semi-definite cone, where  $/$  is applied elementwise,  $\mathbb{E}[s_j]^2 = c^{-1}(\Gamma(c+1/2)/\Gamma(c))^2$  under the SNG prior and  $\mathbb{E}[s_j]^2 = (\pi/2)(\Gamma(2/q)/\sqrt{\Gamma(1/q)\Gamma(3/q)})^2$  under the SPB prior.

## 5 A Numerical Study

In this section we return to the BCI data discussed in Section 1. We are interested in using logistic regression to relate  $n$  indicators  $\mathbf{y}$  of whether or not subjects are viewing a target letter during each of  $n$  trials to an  $n \times p$  matrix  $\mathbf{X}$  of  $n$  multivariate time series of EEG measurements collected at  $p_1 = 208$  time points across  $p_2 = 8$  channels. We focus on a subset of data collected from a single subject using a P300 speller and a gGAMMA.sys EEG device (Forney et al., 2013).

We assume  $\Sigma$  is separable, i.e.  $\Sigma = \Sigma_2 \otimes \Sigma_1$ . The covariance matrices  $\Sigma_1$  and  $\Sigma_2$  characterize relationship of regression coefficients  $\mathbf{B}$  over time and across channels, respectively. Because the scales of  $\Sigma_1$  and  $\Sigma_2$  are not separately identifiable, we assume that the diagonal elements of  $\Sigma_1$  are exactly equal to 1. We also assume that  $\Omega_1$  and  $\Psi_1$  have autoregressive structures of order one, with  $\omega_{1,ij} = \rho_\Omega^{|i-j|}$  and  $\psi_{1,ij} = \rho_\Psi^{|i-j|}$ . We note that the corresponding marginal variance  $\Sigma_1$  is autoregressive of order one under the SPN prior but not the SNG and SPB priors. If  $\Omega_1$  and  $\Psi_1$  have autoregressive structure of order one with parameters  $\rho_\Omega$  and  $\rho_\Psi$ , then  $\Sigma_1$  has autoregressive structure of order one with parameter  $\rho = \rho_\Omega \rho_\Psi$ , whereas the matrix  $\Sigma_1 = \Omega_1 \circ \mathbb{E}[\mathbf{s}\mathbf{s}']$  does not have autoregressive structure of order one. We include an intercept  $\gamma$  in the linear model and assume an improper uniform prior  $\gamma \sim \text{uniform}(-\infty, \infty)$ .

We perform fully Bayes inference, assuming prior distributions for  $\Omega$  and, in the case of the SPN prior,  $\Psi$ . Fully Bayes results are based on assuming  $\Omega_2^{-1} \sim \text{Wishart}(10, \mathbf{I}_8)$ ,  $\rho_\Omega \sim \text{beta}(2, 2)$  and, when using the SPN prior,  $\Psi_2^{-1} \sim \text{Wishart}(10, \mathbf{I}_8)$ ,  $\rho_\Psi \sim \text{beta}(2, 2)$ . We use the latent-variable representation of logistic regression introduced by Polson et al. (2013) to simulate from the full conditional distribution of  $\beta$ , the elliptical slice sampling procedure described in Section 4 to simulate from the full conditional distribution of  $\mathbf{s}$ , and univariate slice sampling to simulate from the full conditional distributions of  $\rho_\Omega$  and  $\rho_\Psi$ . Because latent-variable representation of logistic regression scales poorly in  $n$  and  $p$ , we reduce the number of time points from  $p_2 = 208$  to  $p_1 = 52$  by averaging every four EEG measurements over time. We also set aside the last 100 trials as test data and retain a subset of  $n = 140$  trials for training data, in order to assess out of sample predictive performance.

We simulate 200,000 samples from the posterior distribution and thin by a factor of 2. The remaining 100,000 samples have minimum effective sample sizes for all unknown parameters of 1343.69 under a multivariate normal prior, 115.15 under the SPN prior, 176.26, 185.10, 242.62 and 504.56 under the SNG priors with  $c = 0.3$ ,  $c = 0.5$ ,  $c = 1$  and  $c = 10$ , respectively, and 160.87, 43.23, 48.14 and 779.53 under the SPB prior with  $q = 0.65$ ,  $q = 0.78$ ,  $q = 1$  and  $q = 1.75$ , respectively.

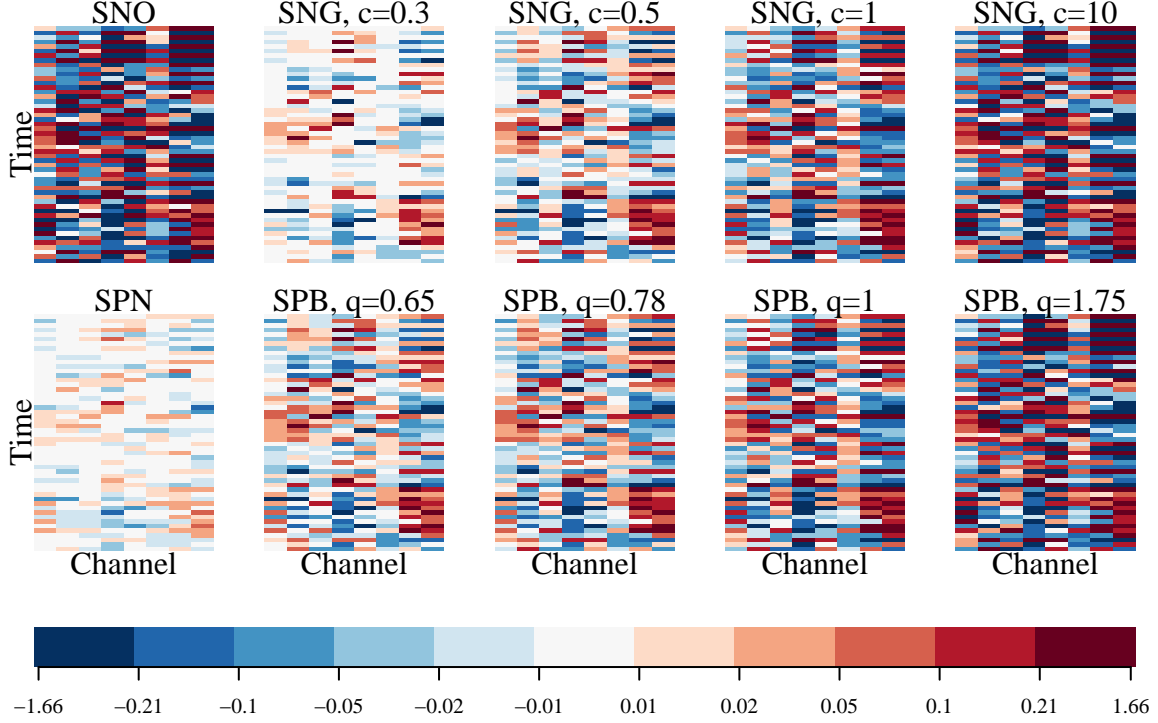


Figure 8: Approximate posterior medians of  $\mathbf{B}$ .

Figure 8 shows posterior median estimates of elements of  $\mathbf{B}$  under a multivariate normal prior (SNO) and nine choices of structured shrinkage priors. The estimated posterior medians are consistent with our expectations; they all display similar structure across channels and over time as well as increasing shrinkage of individual elements of  $\beta$  as  $c, q \rightarrow 0$ .

Figure 9 shows posterior mean estimates of the channel-by-channel correlation matrices corresponding to  $\Sigma_2$  as well as 95% credible interval and posterior mean estimates for the  $\sigma_{1,12}$ , the posterior correlation of two elements of  $\mathbf{B}$  corresponding to consecutive



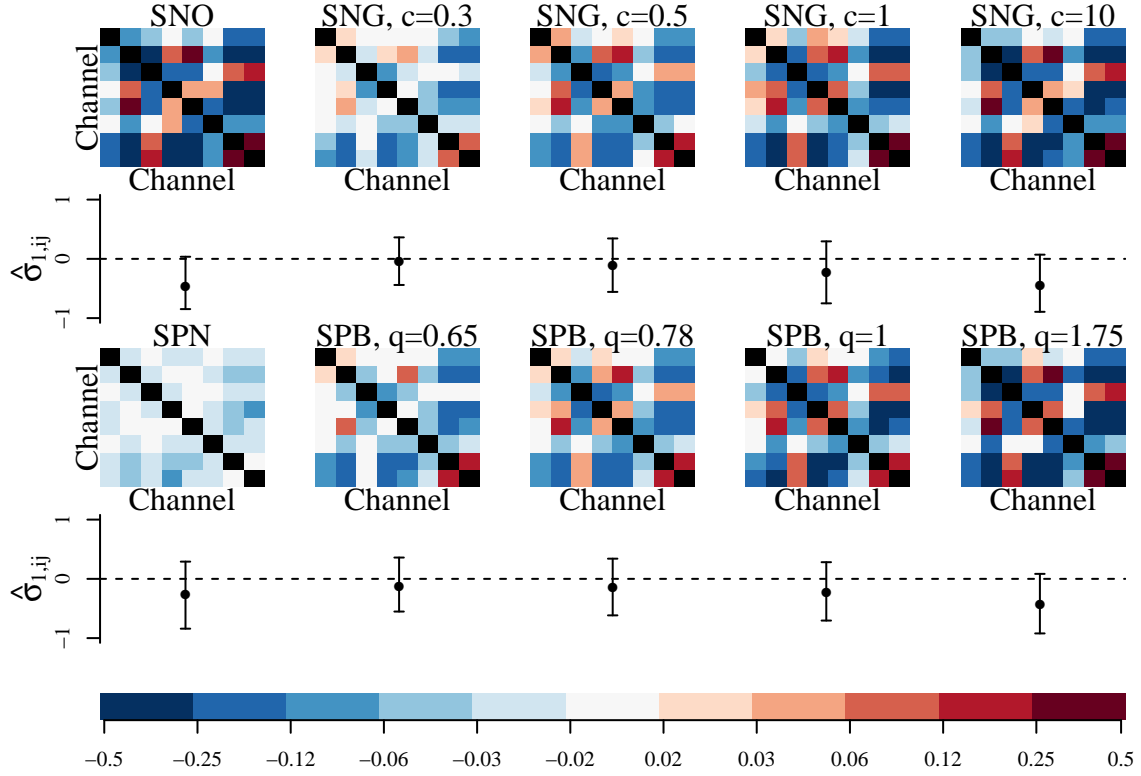


Figure 9: Approximate posterior means and 95% credible intervals for the marginal posterior correlation of consecutive time points  $\sigma_{1,ij}$  with  $|i - j| = 1$  and approximate posterior mean channel-by-channel correlation matrices  $\Sigma_2$ .

time points. Overall, the estimates indicate that there is indeed evidence of dependence across channels and over time, which supports our decision to use structured priors for this problem. Again, these are largely consistent with our expectations; the amount of dependence across channels and over time under the SNG and SPB priors is decreasing as  $c$  or  $q$  decrease and the priors become heavier tailed and encourage sparsity more aggressively.

Interestingly, the SPN prior estimates relatively weak correlations across channels and over time, compared to the other prior distributions. This is surprising because the SPN prior differs from the SNG and SPB priors in that it can accommodate arbitrary dependence structures, however it is likely caused by differences between the induced prior on the correlation of any two elements of  $\beta$  using the fully Bayes implementation SPN versus SPB and SNG priors.

Last, Figure 10 shows ROC curves for the 100 held-out trials based on posterior mean

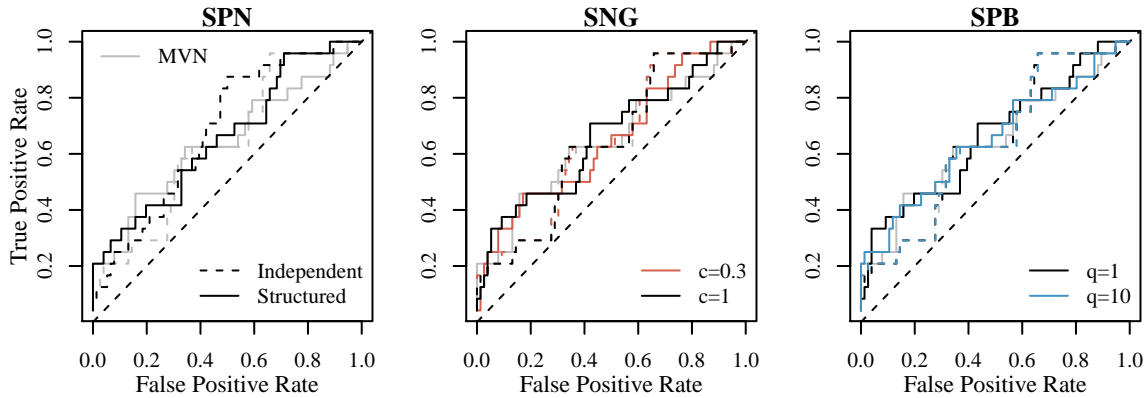


Figure 10: A subset of ROC curves based on posterior mean predictions  $\hat{\mathbf{y}}_{\text{test}}$  compared to their independent counterparts and results from a multivariate normal prior.

predictions  $\hat{\mathbf{y}}_{\text{test}}$ . Here, we include a comparison to the estimates based on the corresponding unstructured priors as well, which assume  $\mathbf{\Omega}$  and  $\mathbf{\Psi} \propto \mathbf{I}_p$ . We observe that the structured priors tend to outperform the independent priors, and that the SHP priors that generalize Laplace or heavier-than-Laplace-tailed priors can yield slightly better performance than a multivariate normal prior especially at thresholds that correspond to low false positive rates. Examining out-of-sample prediction performance by computing the mean misclassification rate, using a cutoff of 0.5 for the predicted values  $\hat{\mathbf{y}}_{\text{test}}$ , yields similar conclusions. The SPN prior performs best, with a misclassification rate of 21%, followed by the multivariate Laplace prior obtained by using the SNG prior with  $c = 1$  or the SPB prior with  $q = 1$ , with a misclassification rate of 22%. In contrast, the multivariate normal prior has a misclassification rate of 26%.

## 6 Discussion

We introduced the SHP class of novel structured shrinkage priors for regression coefficients in generalized linear models. We explored and compared properties of these prior distributions and show that they can encourage both sparsity and structure, which can be difficult to simultaneously model using existing prior distributions. We provide a parsimonious and general approach to posterior mode estimation and full posterior distribution simulation

based on univariate and elliptical slice sampling that allows for straightforward simulation of elements of  $\mathbf{s}$  from nonstandard full conditional distributions. We demonstrate how all three prior distributions can improve interpretability of estimated logistic regression coefficients and out of sample prediction relative to multivariate normal or independent priors P300 speller prediction problem.

This material has several additional applications and extensions. Throughout, we have focused on the development of structured shrinkage prior distributions for regression coefficients in generalized linear models, however the same distributions could be used to model correlated and heavy-tailed errors as in Finegold and Drton (2011), as alternatives to Gaussian process models, or to construct shrinkage priors for other quantities, e.g. covariance matrices (Daniels and Pourahmadi, 2002). Also, the elliptical slice sampling procedure we use to construct a tractable Gibbs sampler for simulating from  $p(\mathbf{s}|\boldsymbol{\beta}, \boldsymbol{\theta})$  under the SPN, SNG and SPB priors can be to perform posterior inference under other novel structured generalizations of *any* shrinkage priors that can be represented using Hadamard products involving a normal random vector. This includes the popular horseshoe prior, as well as others (Polson and Scott, 2010; Bhattacharya et al., 2015). Last, a natural extension to this work would treat  $c$  and  $q$  as unknown under the SNG and SPB priors, respectively. We might perform maximum marginal likelihood estimation of  $c$  or  $q$  or assume prior distributions for  $c$  and  $q$ , the latter at the cost of possibly sparse posterior mode estimates of  $\boldsymbol{\beta}$ .

## Acknowledgements

This work was partially supported by NSF grants DGE-1256082 and DMS-1505136.

## Supplementary Materials

Supplementary material available online includes proofs of all the propositions and additional numerical results. A stand-alone package for implementing the methods described in this paper can be downloaded from <https://github.com/maryclare/sspcomp>.

# References

- Bhattacharya, A., D. Pati, N. S. Pillai, and D. B. Dunson (2015). Dirichlet Laplace Priors for Optimal Shrinkage. *Journal of the American Statistical Association* 110(512), 1479–1490.
- Caron, F. and A. Doucet (2008). Sparse Bayesian Nonparametric Regression. *International Conference on Machine Learning*, 88–95.
- Carvalho, C. M., N. G. Polson, and J. G. Scott (2010). The horseshoe estimator for sparse signals. *Biometrika* 97(2), 465–480.
- Damien, P., J. Wakefield, and S. Walker (1999). Gibbs Sampling for Bayesian Non-Conjugate and Hierarchical Models by Using Auxiliary Variables. *Journal of the Royal Statistical Society. Series B (Statistical Methodology)* 61(2), 331–344.
- Daniels, M. J. and M. Pourahmadi (2002). Bayesian analysis of covariance matrices and dynamic models for longitudinal data. *Biometrika* 89(3), 553–566.
- de Brecht, M. and N. Yamagishi (2012). Combining sparseness and smoothness improves classification accuracy and interpretability. *NeuroImage* 60(2), 1550–1561.
- Dempster, A. P., N. M. Laird, and D. B. Rubin (1977). Maximum likelihood from incomplete data via the EM algorithm. *Journal of the Royal Statistical Society. Series B* 39(1), 1–38.
- Devroye, L. (2009). Random variate generation for exponentially and polynomially tilted stable distributions. *ACM Transactions on Modeling and Computer Simulation* 19(4), 1–20.
- Finegold, M. and M. Drton (2011). Robust graphical modeling of gene networks using classical and alternative t-distributions. *Annals of Applied Statistics* 5(2 A), 1057–1080.
- Forney, E., C. Anderson, P. Davies, W. Gavin, B. Taylor, and M. Roll (2013). A Comparison of EEG Systems for Use in P300 Spellers by Users With Motor Impairments in Real-

- World Environments. *Proceedings of the Fifth International Brain-Computer Interface Meeting*.
- Frank, I. E. and J. H. Friedman (1993). A Statistical View of Some Chemometrics Regression Tools. *Technometrics* 35(2), 109.
- Griffin, J. E. and P. J. Brown (2010). Inference with normal-gamma prior distributions in regression problems. *Bayesian Analysis* 5(1), 171–188.
- Griffin, J. E. and P. J. Brown (2012a). Competing Sparsity: A hierarchical prior for sparse regression with grouped effects. *Manuscript*.
- Griffin, J. E. and P. J. Brown (2012b). Structuring shrinkage: some correlated priors for regression. *Biometrika* 99(2), 481–487.
- Hoff, P. D. (2017). Lasso, fractional norm and structured sparse estimation using a Hadamard product parametrization. *Computational Statistics and Data Analysis* 115, 186–198.
- Kalli, M. and Griffin (2014). Time-varying sparsity in dynamic regression models. *Journal of Econometrics* 178, 779–793.
- Kowal, D. R., D. S. Matteson, and D. Ruppert (2017). Dynamic Shrinkage Processes. *ArXiv preprint. arXiv:1707.00763*, 1–45.
- Kyung, M., J. Gill, M. Ghosh, and G. Casella (2010). Penalized Regression, Standard Errors, and Bayesian Lassos. *Bayesian Analysis* 5(2), 369–412.
- Makeig, S., C. Kothe, T. Mullen, N. Bigdely-Shamlo, Z. Zhang, and K. Kreutz-Delgado (2012). Evolving Signal Processing for Brain Computer Interfaces. *Proceedings of the IEEE* 100(Special Centennial Issue), 1567–1584.
- Murray, I., R. P. Adams, and D. J. C. Mackay (2010). Elliptical slice sampling. *Journal of Machine Learning Research: WCP* 9, 541–548.
- Neal, R. M. (2003). Slice Sampling. *Annals of Statistics* 31(3), 758–767.

- Ng, B. and R. Abugharbieh (2011). Modeling Spatiotemporal Structure in fMRI Brain Decoding Using Generalized Sparse Classifiers. *IEEE International Workshop on Pattern Recognition in NeuroImaging*, 65–68.
- Nishihara, R., I. Murray, and R. P. Adams (2014). Parallel MCMC with Generalized Elliptical Slice Sampling. *Journal of Machine Learning Research* 15(15), 2087–2112.
- Park, T. and G. Casella (2008). The Bayesian Lasso. *Journal of the American Statistical Association* 103(482), 681–686.
- Perry, P. O. (2017). Fast moment-based estimation for hierarchical models. *Journal of the Royal Statistical Society. Series B* 79(1), 267–291.
- Polson, N. G. and J. G. Scott (2010). Shrink Globally, Act Locally: Bayesian Sparsity and Regularization. In J. M. Bernardo, M. J. Bayarri, J. O. Berger, A. P. Dawid, D. Heckerman, A. F. M. Smith, and M. West (Eds.), *Bayesian Statistics 9*, pp. 501–538. Oxford University Press.
- Polson, N. G., J. G. Scott, and J. Windle (2013). Bayesian inference for logistic models using Pólya-Gamma latent variables. *Journal of the American Statistical Association* 108(504), 1339–1349.
- Polson, N. G., J. G. Scott, and J. Windle (2014). The Bayesian bridge. *Journal of the Royal Statistical Society. Series B: Statistical Methodology* 76(4), 713–733.
- Roy, V. and S. Chakraborty (2016). Selection of Tuning Parameters, Solution Paths and Standard Errors for Bayesian Lassos. *Bayesian Analysis* TBA(TBA), 1–26.
- Sharma, N. (2013). *Single-Trial P300 Classification with LDA and Neural Networks*. Ph. D. thesis, Colorado State University.
- Styan, P. H. (1973). Hadamard Products and Multivariate Statistical Analysis. *Linear Algebra and Its Applications* 6, 217–240.
- Tibshirani, R. (1996). Regression Shrinkage and Selection via the Lasso. *Journal of the Royal Statistical Society: Series B (Statistical Methodology)* 58(1), 267–288.

- van Gerven, M., B. Cseke, R. Oostenveld, and T. Heskes (2009). Bayesian Source Localization with the Multivariate Laplace Prior. *Advances in Neural Information Processing Systems 22*, 1–9.
- van Gerven, M. A. J., B. Cseke, F. P. de Lange, and T. Heskes (2010). Efficient Bayesian multivariate fMRI analysis using a sparsifying spatio-temporal prior. *Neuroimage 50*, 150–161.
- Wolpaw, J. and E. W. Wolpaw (2012). *Brain-Computer Interfaces: Principles and Practice*. USA: Oxford University Press.
- Wu, A., M. Park, O. Koyejo, and J. W. Pillow (2014). Sparse Bayesian structure learning with dependent relevance determination prior. *Advances in Neural Information Processing Systems*, 1628–1636.
- Zhao, S., C. Gao, S. Mukherjee, and B. E. Engelhardt (2016). Bayesian group factor analysis with structured sparsity. *Journal of Machine Learning Research 17*, 1–47.

## A Relationship Between $\Omega$ , $\Psi$ and Fourth-Order Prior Cross Moments

Let  $\mathbf{C}_\Omega$  be the correlation matrix corresponding to  $\Omega$ , and recall that parametrize  $\Psi$  as having diagonal elements equal to 1. Off-diagonal elements of  $\mathbf{C}_\Omega$  and  $\Psi$  determine fourth-order cross moments of elements of  $\beta$ . Recalling that the marginal covariance matrix  $\Sigma = \Omega \circ \Psi$  and letting  $\mathbf{C}_\Sigma$  be the correlation matrix corresponding to  $\Sigma$ , we have

$$\begin{aligned} \frac{\mathbb{E}[\beta_j^2 \beta_k^2]}{\sigma_{jj} \sigma_{kk}} &= 1 + 2c_{\Omega,jk}^2 + 2c_{\Psi,jk}^2 + 4c_{\Sigma,jk}^2 & j \neq k \\ \frac{\mathbb{E}[\beta_j^2 \beta_k \beta_l]}{\sigma_{jj} \sqrt{\sigma_{kk} \sigma_{ll}}} &= c_{\Sigma,kl} + 4c_{\Sigma,jk} c_{\Sigma,jl} + 2c_{\Omega,kl} c_{\Psi,jk} c_{\Psi,jl} + 2c_{\Psi,kl} c_{\Omega,jk} c_{\Omega,jl} & j \neq k, j \neq l, k \neq l. \end{aligned}$$

We can see that these fourth-order cross moments depend on the values of *both*  $c_{\Omega,jk}$  and  $c_{\Psi,jk}$ , in addition to their product  $c_{\Sigma,jk}$ .

## B Generalized Gamma Rate Mixture Representation of Polynomially Tilted Positive $\alpha$ -Stable Random Variables

Following Devroye (2009), we can write polynomially titled positive  $\alpha$ -stable  $s_j^2$  as:

$$s_j^2 \stackrel{d}{=} \frac{\Gamma\left(\frac{1}{2\alpha}\right) \xi_j^{\frac{1-\alpha}{\alpha}}}{2\Gamma\left(\frac{3}{2\alpha}\right)}, \quad \xi_j \stackrel{i.i.d.}{\sim} \text{gamma}\left(\text{shape} = \frac{1+\alpha}{2\alpha}, \text{rate} = f(\delta_j|\alpha)\right) \text{ and}$$

$$p(\delta_j|\alpha) \propto f(\delta_j|\alpha)^{\frac{\alpha-1}{2\alpha}},$$

where  $f(\delta_j|\alpha) = \sin(\alpha\delta_j)^{\frac{\alpha}{1-\alpha}} \sin((1-\alpha)\delta_j) / \sin(\delta_j)^{\frac{1}{1-\alpha}}$  and  $\delta_j \in (0, \pi)$ . The density  $f(\delta_j|\alpha)$  is non-standard, however Devroye (2009) provides a following method for simulating from  $\delta_j$  from this distribution.

## C Univariate Marginal Distributions

Intuitively, it is clear from the stochastic representation that the marginal distributions are the same as the corresponding univariate shrinkage prior. We can show this directly as follows. The joint marginal prior distribution of  $\beta$  is

$$p(\beta) = \int p(s) p(\beta/s) \left( \prod_{j=1}^p \frac{1}{|s_j|} \right) ds_1 \dots ds_p$$

Then  $p(\beta_1)$  is given by

$$\begin{aligned} p(\beta_1) &= \int p(\beta_1/s_1) p(\beta_{-1}/s_{-1}|\beta_1/s_1) \left( \prod_{j=1}^p \frac{p(s_j)}{|s_j|} \right) ds_1 \dots ds_p d\beta_2 \dots d\beta_p \\ &= \int p(\beta_1/s_1) p(s_1)/|s_1| \underbrace{\left( \int p(\beta_{-1}/s_{-1}|\beta_1/s_1) \left( \prod_{j=2}^p \frac{p(s_j)}{|s_j|} \right) ds_2 \dots ds_p d\beta_2 \dots d\beta_p \right)}_{(*)} ds_1. \end{aligned}$$

The term  $(*)$  is equal to  $\int p(\beta_{-1}|\beta_1/s_1) d\beta_2 \dots d\beta_p$ . This is the integral of a density, and accordingly  $(*) = 1$  and  $p(\beta_1) = \int p(\beta_1/s_1) p(s_1)/|s_1| ds_1$ .



## D Proofs of Propositions

### D.1 Propositions 2.1 and 2.3

First, we prove the following lemma:

**Lemma D.1** For  $\alpha > 0$  and  $\gamma \in \mathbb{R}$ ,  $\int_{-\infty}^{\infty} \frac{1}{|s|} \exp\{-\alpha(s^2 - \gamma s)\} ds = +\infty$ .

First let's consider this integral when  $\gamma > 0$ :

$$\begin{aligned} \int_{-\infty}^{\infty} \frac{1}{|s|} \exp\{-\alpha(s^2 - \gamma s)\} ds &= \int_{-\infty}^0 -\frac{1}{s} \exp\{-\alpha s\}^{s-\gamma} ds + \\ &\quad \int_0^{\gamma} \frac{1}{s} \exp\{-\alpha s\}^{s-\gamma} ds + \int_{\gamma}^{\infty} \frac{1}{s} \exp\{-\alpha s\}^{s-\gamma} ds. \end{aligned}$$

Because the integrand is nonnegative for all  $s$ , if *any* of these terms evaluate to  $+\infty$ , the entire integral evaluates to  $+\infty$ . Let's examine the middle integral. Note that over this range,  $s - \gamma \leq 0$ ,  $\exp\{-\alpha s\} \leq 1$  and accordingly,  $\exp\{-\alpha s\}^{s-\gamma} \geq 1$ .

$$\begin{aligned} \int_0^{\gamma} \frac{1}{s} \exp\{-\alpha s\}^{s-\gamma} ds &\geq \int_0^{\gamma} \frac{1}{s} ds \\ &= (\ln(\gamma) - \lim_{a \rightarrow 0^+} \ln(a)) = +\infty. \end{aligned}$$

Now let's consider the same integral when  $\gamma < 0$ :

$$\begin{aligned} \int_{-\infty}^{\infty} \frac{1}{|s|} \exp\{-\alpha(s^2 - \gamma s)\} ds &= \int_{-\infty}^{\gamma} -\frac{1}{s} \exp\{-\alpha s\}^{s-\gamma} ds + \\ &\quad \int_{\gamma}^0 -\frac{1}{s} \exp\{-\alpha s\}^{s-\gamma} ds + \int_0^{\infty} \frac{1}{s} \exp\{-\alpha s\}^{s-\gamma} ds. \end{aligned}$$

Again, if *any* of these terms evaluate to  $+\infty$ , the entire integral evaluates to  $+\infty$ . Again, let's consider the middle term. Over this interval,  $\exp\{-\alpha s\} \geq 1$  and  $s - \gamma \geq 0$ . It follows that  $\exp\{-\alpha s\}^{s-\gamma} \geq 1$  and:

$$\begin{aligned} \int_{\gamma}^0 -\frac{1}{s} \exp\{-\alpha s\}^{s-\gamma} ds &\geq \int_{\gamma}^0 -\frac{1}{s} ds \\ &= \int_0^{-\gamma} \frac{1}{s} ds = +\infty. \end{aligned}$$

Now we'll consider one last case where  $\gamma = 0$ :

$$\int_{-\infty}^{\infty} \frac{1}{|s|} \exp\{-\alpha s^2\} ds = \int_{-\infty}^0 -\frac{1}{s} \exp\{-\alpha s^2\} ds + \int_0^{1/\sqrt{\alpha}} \frac{1}{s} \exp\{-\alpha s^2\} ds + \int_{1/\sqrt{\alpha}}^{\infty} \frac{1}{s} \exp\{-\alpha s^2\} ds.$$

As in the previous cases, *any* of these terms evaluate to  $+\infty$ , the entire integral evaluates to  $+\infty$ . Examining the middle term one last time, we have:

$$\begin{aligned}
\int_0^{1/\sqrt{\alpha}} \frac{1}{s} \exp\{-\alpha s^2\} ds &\geq \int_0^{1/\sqrt{\alpha}} \frac{1}{s} \exp\{-\sqrt{\alpha}s\} ds \\
&\geq \int_0^{1/\sqrt{\alpha}} \frac{1 - \sqrt{\alpha}s}{s} ds \\
&= \int_0^{1/\sqrt{\alpha}} \frac{1}{s} ds - \int_0^{1/\sqrt{\alpha}} \alpha ds \\
&= \ln(1/\sqrt{\alpha}) - \lim_{a \rightarrow 0+} \ln(a) - \sqrt{\alpha} = +\infty.
\end{aligned}$$

### D.1.1 Proof of Proposition 2.1:

Now we can evaluate the marginal density  $p(\boldsymbol{\beta} = \mathbf{b} | \boldsymbol{\Omega}, \boldsymbol{\Psi})$  when  $b_j = 0$  for some  $j \in \{1, \dots, p\}$ . Without loss of generality, set  $\beta_1 = 0$ . Letting  $\mathbf{b}_{-1}$  and  $\mathbf{s}_{-1}$  refer to the vectors  $\mathbf{b}$  and  $\mathbf{s}$  each with the first element removed,  $(\boldsymbol{\Omega}^{-1})_{-1,-1}$  be the matrix  $\boldsymbol{\Omega}^{-1}$  with the first row and column removed,  $(\boldsymbol{\Psi}^{-1})_{-1,-1}$  be the matrix  $\boldsymbol{\Psi}^{-1}$  with the first row and column removed and  $(\boldsymbol{\Psi}^{-1})_{-1,1}$  be the first column of  $\boldsymbol{\Psi}^{-1}$  excluding the first element. For  $\mathbf{b} = (0, \mathbf{b}_{-1})$ ,

$$\begin{aligned}
p((0, \mathbf{b}_{-1}) | \boldsymbol{\Psi}, \boldsymbol{\Omega}) &\propto \int \frac{1}{\prod_{i=1}^p |s_i|} \exp\left\{-\frac{1}{2} (\mathbf{b}' \text{diag}\{\mathbf{1}/\mathbf{s}\} \boldsymbol{\Omega}^{-1} \text{diag}\{\mathbf{1}/\mathbf{s}\} \mathbf{b} + \mathbf{s}' \boldsymbol{\Psi}^{-1} \mathbf{s})\right\} ds \\
&= \int \frac{1}{\prod_{i=2}^p |s_i|} \exp\left\{-\frac{1}{2} (\mathbf{b}'_{-1} \text{diag}\{\mathbf{1}/\mathbf{s}_{-1}\} (\boldsymbol{\Omega}^{-1})_{-1,-1} \text{diag}\{\mathbf{1}/\mathbf{s}_{-1}\} \mathbf{b}_{-1} + \mathbf{s}'_{-1} (\boldsymbol{\Psi}^{-1})_{-1,-1} \mathbf{s}_{-1})\right\} \\
&\quad \underbrace{\int_{-\infty}^{\infty} \frac{1}{|s_1|} \exp\left\{-\frac{1}{2} (s_1^2 (\boldsymbol{\Psi}^{-1})_{11} - 2s_1 (\boldsymbol{\Psi}^{-1})'_{-1,1} \mathbf{s}_{-1})\right\} ds_1}_{(*)} ds_{-1}.
\end{aligned}$$

Applying Lemma D.1, the term denoted by  $(*)$  evaluates to  $+\infty$  for every value of  $\mathbf{s}_{-1}$ .

### D.1.2 Proof of Proposition 2.3:

Proposition 2.3 follows from Proposition 2.1 and Lemma D.1. Again, letting  $\beta_1 = 0$ , for  $\boldsymbol{\beta} = (0, \boldsymbol{\beta}_{-1})$ ,

$$\begin{aligned}
p(\beta_1 = 0 | \boldsymbol{\Psi}, \boldsymbol{\Omega}) &\propto \int \frac{1}{\prod_{i=1}^p |s_i|} \exp\left\{-\frac{1}{2} (\boldsymbol{\beta}' \text{diag}\{\mathbf{1}/\mathbf{s}\} \boldsymbol{\Omega}^{-1} \text{diag}\{\mathbf{1}/\mathbf{s}\} \boldsymbol{\beta} + \mathbf{s}' \boldsymbol{\Psi}^{-1} \mathbf{s})\right\} ds d\boldsymbol{\beta}_{-1} \\
&= \int \frac{1}{\prod_{i=2}^p |s_i|} \exp\left\{-\frac{1}{2} (\boldsymbol{\beta}'_{-1} \text{diag}\{\mathbf{1}/\mathbf{s}_{-1}\} (\boldsymbol{\Omega}^{-1})_{-1,-1} \text{diag}\{\mathbf{1}/\mathbf{s}_{-1}\} \boldsymbol{\beta}_{-1} + \mathbf{s}'_{-1} (\boldsymbol{\Psi}^{-1})_{-1,-1} \mathbf{s}_{-1})\right\} \\
&\quad \underbrace{\int_{-\infty}^{\infty} \frac{1}{|s_1|} \exp\left\{-\frac{1}{2} (s_1^2 (\boldsymbol{\Psi}^{-1})_{11} - 2s_1 (\boldsymbol{\Psi}^{-1})'_{-1,1} \mathbf{s}_{-1})\right\} ds_1}_{(*)} ds_{-1} d\boldsymbol{\beta}_{-1}.
\end{aligned}$$

Again,  $(*)$  evaluates to  $+\infty$  for any value of  $\mathbf{s}_{-1}$  and does not depend at all on  $\boldsymbol{\beta}_{-1}$ .

## D.2 Proofs of Propositions 2.2 and 2.4

First, we prove the following lemma:

**Lemma D.2** For  $0 < c < 1/2$ ,  $\int_0^\infty (s^2)^{c-1/2-1} \exp\{-cs^2\} ds^2 = +\infty$ .

We can break the integral into two nonnegative components, as follows:

$$\int_0^\infty (s^2)^{c-1/2-1} \exp\{-cs^2\} ds^2 = \int_0^{1/c} (s^2)^{c-1/2-1} \exp\{-cs^2\} ds^2 + \int_{1/c}^\infty (s^2)^{c-1/2-1} \exp\{-cs^2\} ds^2.$$

Now let's examine the first component. When  $s^2 < 1/c$ ,  $\exp\{-cs^2\} \geq 1 - cs^2$  and

$$\begin{aligned} \int_0^{1/c} (s^2)^{c-1/2-1} \exp\{-cs^2\} ds^2 &\geq \int_0^{1/c} (s^2)^{c-1/2-1} (1 - cs^2) ds^2 \\ &= \int_0^{1/c} (s^2)^{c-1/2-1} ds^2 - c \int_0^{1/c} (s^2)^{c-1/2} ds^2 \\ &= \frac{(1/c)^{c-1/2}}{c-1/2} - \frac{1}{c-1/2} \lim_{a \rightarrow 0} a^{c-1/2} - c \frac{(1/c)^{c-1/2+1}}{c-1/2+1} + \\ &\quad \frac{c}{c-1/2+1} \underbrace{\lim_{a \rightarrow 0} a^{c-1/2+1}}_{=0 \text{ for } c>0} \\ &= \begin{cases} +\infty & 0 < c < 1/2 \\ \frac{(1/c)^{c-1/2}}{c-1/2} - \frac{1}{c-1/2} \mathbb{1}_{\{c=1/2\}} - \frac{(1/c)^{c-1/2}}{c-1/2+1} & c \geq 1/2 \end{cases} \end{aligned}$$

### D.2.1 Proof of Proposition 2.2

Now we can evaluate the marginal density  $p(\boldsymbol{\beta} = \mathbf{b}|c, \boldsymbol{\Omega})$  when  $b_j = 0$  for some  $j \in \{1, \dots, p\}$ . Without loss of generality, set  $\beta_1 = 0$ . Letting  $\mathbf{b}_{-1}$  and  $\mathbf{s}_{-1}$  refer to the vectors  $\mathbf{b}$  and  $\mathbf{s}$  each with the first element removed and  $(\boldsymbol{\Omega}^{-1})_{-1,-1}$  be the matrix  $\boldsymbol{\Omega}^{-1}$  with the first row and column removed. For  $\mathbf{b} = (0, \mathbf{b}_{-1})$ ,

$$\begin{aligned} p((\beta_1 = 0, \mathbf{b}_{-1})|c, \boldsymbol{\Omega}) &\propto \int \frac{(s_1^2)^{c-1}}{\prod_{i=1}^p s_i} \exp \left\{ -\frac{1}{2} (\mathbf{b}' \text{diag}\{\mathbf{1}/\mathbf{s}\} \boldsymbol{\Omega}^{-1} \text{diag}\{\mathbf{1}/\mathbf{s}\} \mathbf{b}) - \sum_{j=1}^p cs_j^2 \right\} d\mathbf{s} \\ &= \int \left( \prod_{j=2}^p (s_j^2)^{c-1/2-1} \right) \exp \left\{ -\frac{1}{2} (\mathbf{b}_{-1}' \text{diag}\{\mathbf{1}/\mathbf{s}_{-1}\} (\boldsymbol{\Omega}^{-1})_{-1,-1} \text{diag}\{\mathbf{1}/\mathbf{s}_{-1}\} \mathbf{b}_{-1}) - \sum_{j=2}^p cs_j^2 \right\} \\ &\quad \underbrace{\int_0^\infty (s_1^2)^{c-1/2-1} \exp\{-cs_1^2\} ds_1}_{(*)} d\mathbf{s}_{-1}. \end{aligned}$$

Applying Lemma D.2, the term denoted by  $(*)$  evaluates to  $+\infty$  for every value of  $\mathbf{s}_{-1}$ .

### D.2.2 Proof of Proposition 2.4

Proposition 2.4 follows from Proposition 2.2 and Lemma D.2. For  $\beta = (0, \beta_{-1})$ ,

$$\begin{aligned}
p(\beta_1 = 0 | c, \Omega) &\propto \int \frac{(s_i^2)^{c-1}}{\prod_{i=1}^p s_i} \exp \left\{ -\frac{1}{2} (\beta' \text{diag} \{1/s\} \Omega^{-1} \text{diag} \{1/s\} \beta) - \sum_{j=1}^p c s_j^2 \right\} d\mathbf{s} d\beta_{-1} \\
&= \int \left( \prod_{j=2}^p (s_j^2)^{c-1/2-1} \right) \exp \left\{ -\frac{1}{2} (\beta'_{-1} \text{diag} \{1/s_{-1}\} (\Omega^{-1})_{-1,-1} \text{diag} \{1/s_{-1}\} \beta_{-1}) - \sum_{j=2}^p c s_j^2 \right\} \\
&\quad \underbrace{\int_0^\infty (s_1^2)^{c-1/2-1} \exp \{-c s_1^2\} ds_1}_{(*)} d\mathbf{s}_{-1} d\beta_{-1}.
\end{aligned}$$

Again,  $(*)$  evaluates to  $+\infty$  for any value of  $\mathbf{s}_{-1}$  and does not depend at all on  $\beta_{-1}$ .

## E Kurtosis of SHP $\beta_j$

### E.1 SNG $\beta_j$

When  $s_j^2 \sim \text{gamma}(c, c)$ , we have:

$$\begin{aligned}
\int_0^\infty s_j^4 \frac{c^c}{\Gamma(c)} (s_j^2)^{c-1} \exp \{-c s_j^2\} ds_j^2 &= \frac{c^c}{\Gamma(c)} \int_0^\infty (s_j^2)^{c+2-1} \exp \{-c s_j^2\} ds_j^2 \\
&= \left( \frac{c^c \Gamma(c+2)}{c^{c+2} \Gamma(c)} \right) \\
&= c^{-2} (\Gamma(c+2) / \Gamma(c)) \\
&= (c+1) / c.
\end{aligned}$$

A standard normal random variable has  $\mathbb{E}[z_j^4] = 3$ . It follows that

$$\mathbb{E}[\beta_j^4] / \mathbb{E}[\beta_j^2]^2 = 3(c+1) / c.$$

### E.2 SPB $\beta_j$

The kurtosis of a random variable is not a function of the overall scale, so without loss of generality, let  $\mathbb{V}[\beta_j] = 1$ . When  $\beta$  is distributed according to an *SPB* prior, elements  $\beta_j$

each have a power/bridge distribution with density

$$p(\beta_j|q) = \left(\frac{q}{2}\right) \sqrt{\frac{\Gamma(3/q)}{\Gamma(1/q)^3}} \exp \left\{ - \left(\frac{\Gamma(3/q)}{\Gamma(1/q)}\right)^{q/2} |\beta_j|^q \right\}.$$

It follows that

$$\begin{aligned} \mathbb{E}[\beta_j^{2k}] &= \int_{-\infty}^{\infty} \left(\frac{q}{2}\right) \sqrt{\frac{\Gamma(3/q)}{\Gamma(1/q)^3}} \beta_j^{2k} \exp \left\{ - \left(\frac{\Gamma(3/q)}{\Gamma(1/q)}\right)^{q/2} |\beta_j|^q \right\} d\beta_j \\ &= \int_0^{\infty} q \sqrt{\frac{\Gamma(3/q)}{\Gamma(1/q)^3}} \beta_j^{2k} \exp \left\{ - \left(\frac{\Gamma(3/q)}{\Gamma(1/q)}\right)^{q/2} \beta_j^q \right\} d\beta_j \\ &= \int_0^{\infty} \sqrt{\frac{\Gamma(3/q)}{\Gamma(1/q)^3}} \gamma_j^{(2k+1)/q-1} \exp \left\{ - \left(\frac{\Gamma(3/q)}{\Gamma(1/q)}\right)^{q/2} \gamma_j \right\} d\gamma_j, \quad \gamma_j = \beta_j^q, \quad \gamma_j^{1/q} = \beta_j \\ &= \sqrt{\frac{\Gamma(3/q)}{\Gamma(1/q)^3}} \left( \frac{\Gamma((2k+1)/q)}{\left(\frac{\Gamma(3/q)}{\Gamma(1/q)}\right)^{(2k+1)/2}} \right) \\ &= \Gamma(3/q)^{(-2k)/2} \Gamma(1/q)^{(2k-2)/2} \Gamma((2k+1)/q). \end{aligned}$$

It follows that the kurtosis of  $\beta_j$  is

$$\begin{aligned} \frac{\mathbb{E}[\beta_j^4]}{\mathbb{E}[\beta_j^2]^2} &= \frac{\Gamma(3/q)^{(-4)/2} \Gamma(1/q)^{(4-2)/2} \Gamma((4+1)/q)}{\Gamma(3/q)^{-2} \Gamma(1/q)^{2-2} \Gamma((2+1)/q)^2} \\ &= \frac{\Gamma(1/q) \Gamma(5/q)}{\Gamma(3/q)^2}. \end{aligned}$$

## F Expectation of $s_j$

### F.1 SNG $\beta_j$ with $\mathbb{V}[\beta_j] = 1$

When  $s_j^2 \sim \text{gamma}(c, c)$ , we have:

$$\begin{aligned} \int_0^{\infty} s_j \frac{c^c}{\Gamma(c)} (s_j^2)^{c-1} \exp\{-cs_j^2\} ds_j^2 &= \frac{c^c}{\Gamma(c)} \int_0^{\infty} (s_j^2)^{c+1/2-1} \exp\{-cs_j^2\} ds_j^2 \\ &= \left( \frac{c^c \Gamma(c+1/2)}{c^{c+1/2} \Gamma(c)} \right) \\ &= c^{-1/2} (\Gamma(c+1/2) / \Gamma(c)) \end{aligned}$$

## F.2 SPB $\beta_j$ with $\mathbb{V}[\beta_j] = 1$

This is a little challenging because working with the stable distribution directly is difficult. However, given knowledge of normal moments and the marginal distribution of  $\beta$ , we can “back out”  $\mathbb{E}[s]$ . Let  $\beta = sz$ , where  $z$  is a standard normal random variable and  $1/s^2$  has an  $\alpha$ -stable distribution on the positive real line. When the stable prior is parametrized to yield  $\mathbb{E}[\beta^2] = 1$ , we have:

$$p(\beta|q) = \left(\frac{q}{2}\right) \sqrt{\frac{\Gamma(3/q)}{\Gamma(1/q)^3}} \exp \left\{ - \left( \frac{\Gamma(3/q)}{\Gamma(1/q)} \right)^{q/2} |\beta|^q \right\}.$$

Now, to determine  $\mathbb{E}[s]$ , note that  $\mathbb{E}[|\beta|] = \mathbb{E}[s]\mathbb{E}[|z|]$ . We have

$$\begin{aligned} \mathbb{E}[|\beta|] &= 2 \int_0^\infty \beta p(\beta|q) d\beta \\ &= q \sqrt{\frac{\Gamma(3/q)}{\Gamma(1/q)^3}} \int_0^\infty \beta \exp \left\{ - \left( \frac{\Gamma(3/q)}{\Gamma(1/q)} \right)^{q/2} \beta^q \right\} d\beta \\ &= \left( \sqrt{\frac{\Gamma(3/q)}{\Gamma(1/q)^3}} \right) \left( \frac{\Gamma(2/q) \Gamma(1/q)}{\Gamma(3/q)} \right) \\ &= \frac{\Gamma(2/q)}{\sqrt{\Gamma(1/q) \Gamma(3/q)}}. \end{aligned}$$

According to Wikipedia,  $\mathbb{E}[|z|] = \sqrt{2/\pi}$ . It follows that

$$\mathbb{E}[s] = \sqrt{\frac{\pi}{2}} \left( \frac{\Gamma(2/q)}{\sqrt{\Gamma(1/q) \Gamma(3/q)}} \right).$$

## G Prior Conditional Distributions of $s_j^2$ and $s_j$

### G.1 SPB $\beta_j$

When using the SPB prior, we have  $s_j^2 \stackrel{d}{=} \Gamma(1/(2\alpha)) \xi_j^{\frac{1-\alpha}{\alpha}} / (2\Gamma(3/(2\alpha)))$ , where  $\xi_j \sim \text{gamma}((1+\alpha)/(2\alpha), f(\delta_j|\alpha))$  and  $p(\delta_j|\alpha) \propto f(\delta_j|\alpha)^{\frac{\alpha-1}{2\alpha}}$  on  $(0, \pi)$ . We want to compute the prior con-

ditional distribution  $\pi(s_j^2|\delta_j, \alpha)$  for use in the elliptical slice sampler for  $\mathbf{s}$ . We have:

$$\begin{aligned} s_j^2 &\stackrel{d}{=} \Gamma(1/(2\alpha)) \xi_j^{\frac{1-\alpha}{\alpha}} / (2\Gamma(3/(2\alpha))) \\ &= \left( (\Gamma(1/(2\alpha)) / (2\Gamma(3/(2\alpha))))^{\frac{\alpha}{1-\alpha}} \xi_j \right)^{\frac{1-\alpha}{\alpha}} \\ &\stackrel{d}{=} \tilde{\xi}_j^{\frac{1-\alpha}{\alpha}}, \quad \tilde{\xi}_j \sim \text{gamma} \left( \frac{1+\alpha}{2\alpha}, \left( \frac{2\Gamma(\frac{3}{2\alpha})}{\Gamma(\frac{1}{2\alpha})} \right)^{\frac{\alpha}{1-\alpha}} f(\delta_j|\alpha) \right) \end{aligned}$$

We can find the density of  $s_j^2$  via change of variables. We have

$$\tilde{\xi}_j = (s_j^2)^{\frac{\alpha}{1-\alpha}}, \quad d\tilde{\xi}_j = \left( \frac{\alpha}{1-\alpha} \right) (s_j^2)^{\frac{\alpha}{1-\alpha}-1} ds_j^2.$$

Then the prior conditional distribution is

$$\begin{aligned} \pi(s_j^2|\delta_j, \alpha) &\propto \left( (s_j^2)^{\frac{\alpha}{1-\alpha}} \right)^{\frac{1+\alpha}{2\alpha}-1} (s_j^2)^{\frac{\alpha}{1-\alpha}-1} \exp \left\{ - \left( \frac{2\Gamma(\frac{3}{2\alpha}) s_j^2}{\Gamma(\frac{1}{2\alpha})} \right)^{\frac{\alpha}{1-\alpha}} f(\delta_j|\alpha) \right\} \\ &= (s_j^2)^{\frac{1+\alpha}{2(1-\alpha)}-1} \exp \left\{ - \left( \frac{2\Gamma(\frac{3}{2\alpha}) s_j^2}{\Gamma(\frac{1}{2\alpha})} \right)^{\frac{\alpha}{1-\alpha}} f(\delta_j|\alpha) \right\}. \end{aligned}$$

In practice, we end up working with  $s_j$ , so once more

$$\pi(s_j|\delta_j, \alpha) \propto s_j^{\frac{1+\alpha}{1-\alpha}-1} \exp \left\{ - \left( \frac{2\Gamma(\frac{3}{2\alpha}) s_j^2}{\Gamma(\frac{1}{2\alpha})} \right)^{\frac{\alpha}{1-\alpha}} f(\delta_j|\alpha) \right\}.$$

## G.2 SNG Prior $\beta_j$

Under the SNG prior, we have

$$\pi(s_j^2|c) \propto (s_j^2)^{c-1} \exp \{ -s_j^2 c \}.$$

In practice, we end up working with  $s_j$ , which has the density

$$\pi(s_j|c) \propto (s_j)^{2c-1} \exp \{ -s_j^2 c \}.$$

## H Maximum correlation for bivariate SHP $\beta$

### H.1 SNG $\beta$

Consider  $\mathbf{\Omega} = (1 - \omega)\mathbf{I}_2 + \omega\mathbf{1}_2\mathbf{1}_2'$ . When  $s_j^2 \sim \text{gamma}(c, c)$ , we have:

$$\mathbf{\Sigma} = \begin{pmatrix} 1 & \omega c^{-1} (\Gamma(c + 1/2) / \Gamma(c))^2 \\ \omega c^{-1} (\Gamma(c + 1/2) / \Gamma(c))^2 & 1 \end{pmatrix},$$

where  $|\omega| \leq 1$  by positive semidefiniteness of  $\mathbf{\Omega}$ . It follows that for fixed  $c$ , the largest possible value of  $|\rho|$  is  $(\Gamma(c + 1/2) / \Gamma(c))^2 / c$ .

### H.2 SPB $\beta$

Consider  $\mathbf{\Omega} = (1 - \omega)\mathbf{I}_2 + \omega\mathbf{1}_2\mathbf{1}_2'$ . We have:

$$\mathbf{\Sigma} = \begin{pmatrix} 1 & \omega \left(\frac{\pi}{2}\right) \left(\frac{\Gamma(2/q)}{\sqrt{\Gamma(1/q)\Gamma(3/q)}}\right)^2 \\ \omega \left(\frac{\pi}{2}\right) \left(\frac{\Gamma(2/q)}{\sqrt{\Gamma(1/q)\Gamma(3/q)}}\right)^2 & 1 \end{pmatrix},$$

where  $|\omega| \leq 1$  by positive semidefiniteness of  $\mathbf{\Omega}$ . It follows that for fixed  $q$ , the largest possible value of  $|\rho|$  is  $(\frac{\pi}{2}) \left(\frac{\Gamma(2/q)}{\sqrt{\Gamma(1/q)\Gamma(3/q)}}\right)^2$ .

## I Posterior Simulation Details

### I.1 Univariate Slice Sampling

In several places in this paper, we use a univariate slice sampling algorithm described in Neal (2003) to simulate values of a random variable  $x \in [a, b]$  with density proportional to  $\exp\{g(x)\}$ . Given a previous value  $\tilde{x}$ , we can simulate a new value  $\tilde{x}'$  from a full conditional using univariate slice sampling as follows:

1. Draw  $e \sim \exp(1)$ .
2. Draw  $d \sim \text{uniform}(a, b)$ .
  - If  $g(\tilde{x}) - e \leq g(d)$ , set  $\tilde{x}' = d$ .



- If  $g(\tilde{x}) - e > g(d)$ :

(a) If  $d < \tilde{x}$ , set  $a = d$ , else if  $d \geq \tilde{x}$  set  $b = d$ .

(b) Return to 3.

## I.2 Simulation from Full Conditional Distribution for $\delta_j$

When using the SPB prior, we have  $s_j^2 \stackrel{d}{=} \Gamma(1/(2\alpha))\xi_j^{\frac{1-\alpha}{\alpha}}/(2\Gamma(3/(2\alpha)))$ , where  $\xi_j \sim \text{gamma}((1+\alpha)/(2\alpha), f(\delta_j|\alpha))$  and  $p(\delta_j|\alpha) \propto f(\delta_j|\alpha)^{\frac{\alpha-1}{2\alpha}}$  on  $(0, \pi)$ . Suppose  $s_j^2$  is fixed. Then  $\xi_j = (2\Gamma(3/(2\alpha))s_j^2/\Gamma(1/(2\alpha)))^{\frac{\alpha}{1-\alpha}}$ . Then we can write the full conditional distribution of  $\delta_j$  as

$$\begin{aligned} p(\delta_j|\xi_j, q) &\propto f(\delta_j|\alpha)^{\frac{1+\alpha}{2\alpha}} \exp\{-f(\delta_j|\alpha)\xi_j\} f(\delta_j|\alpha)^{\frac{\alpha-1}{2\alpha}} \\ &= f(\delta_j|\alpha) \exp\{-f(\delta_j|\alpha)\xi_j\}. \end{aligned}$$

Apply the univariate slice sampling algorithm described in Section I.1 using  $g(x) = \log(f(x|\alpha)) - f(x|\alpha)\xi_j$  and initial values  $a = 0$  and  $b = \pi$ .

## I.3 Simulation from Full Conditional Distribution for $\rho$

In the real data application, I consider the setting where  $\mathbf{B}$  and  $\mathbf{S}$  are  $p_1 \times p_2$  matrices and  $\boldsymbol{\beta} = \text{vec}(\mathbf{B}/\mathbf{S})$  has covariance matrix  $\mathbb{V}[\boldsymbol{\beta}/\mathbf{s}] = \boldsymbol{\Omega}_2 \otimes \boldsymbol{\Omega}_1$ , where  $\boldsymbol{\Omega}_1$  is depends on a single autoregressive parameter,  $\rho$ , with  $\omega_{1,ij} = \rho^{|i-j|}$ . The full conditional distribution of  $\rho$  is:

$$\begin{aligned} p(\rho|-) &\propto |\boldsymbol{\Omega}_1|^{-\frac{p_2}{2}} \exp\left\{-\frac{1}{2}\text{tr}(\boldsymbol{\Omega}_1^{-1}(\mathbf{B}/\mathbf{S})\boldsymbol{\Omega}_2^{-1}(\mathbf{B}/\mathbf{S}))\right\} \\ &= (1 - \rho^2)^{-\frac{(p_1-1)p_2}{2}} \exp\left\{-\frac{1}{2}\text{tr}(\boldsymbol{\Omega}_1^{-1}(\mathbf{B}/\mathbf{S})\boldsymbol{\Omega}_2^{-1}(\mathbf{B}/\mathbf{S}))\right\} \pi(\rho), \end{aligned}$$

where elements of  $\boldsymbol{\Omega}_1^{-1}$  are given by

$$\begin{aligned} \omega_1^{11} &= \omega_1^{pp} = (1 - \rho^2)^{-1} \\ \omega_1^{jj} &= (1 - \rho^2)^{-1} (1 + \rho^2) & j \neq 1, j \neq p \\ \omega_1^{jk} &= -\rho (1 - \rho^2)^{-1} & |j - k| = 1 \end{aligned}$$

and  $\pi(\rho)$  is the density of an assumed prior distribution for  $\rho$ . We assume a uniform prior on  $(-1, 1)$ , i.e.  $\text{beta}(1, 1)$  prior for  $(\rho + 1)/2$ .

## I.4 Coordinate Descent for $\mathbf{s}$

For any element of  $\mathbf{s}$ , the

$$\kappa_1 s_j^{-2} + \kappa_2 s_j^{-1} + \kappa_3 \log(s_j^2) + \kappa_4 s_j + \kappa_5 s_j^{\kappa_6}, \kappa_6 \neq 1$$

The optimal value of  $s$  will satisfy

$$-2\kappa_1 s_j^{-3} - \kappa_2 s_j^{-2} + 2\kappa_3 s_j^{-1} + \kappa_4 + \kappa_5 \kappa_6 s_j^{\kappa_6-1} = 0$$

$$-2\kappa_1 - \kappa_2 s_j + 2\kappa_3 s_j^2 + \kappa_4 s_j^3 + \kappa_5 \kappa_6 s_j^{\kappa_6+2} = 0$$

When  $\kappa_6$  is an integer (as is the case for the SNG and SPN priors) we can find all values of  $s$  that satisfy this quickly and exactly using fast polynomial root finding functions from the `polynom` package for R.

When  $\kappa_6$  is *not* an integer, find values of  $s_F$  and  $s_C$  that maximize

$$\kappa_1 s_j^{-2} + \kappa_2 s_j^{-1} + \kappa_3 \log(s_j^2) + \kappa_4 s_j + \kappa_5 s_j^{\text{floor}(\kappa_6)} \text{ and}$$

$$\kappa_1 s_j^{-2} + \kappa_2 s_j^{-1} + \kappa_3 \log(s_j^2) + \kappa_4 s_j + \kappa_5 s_j^{\text{ceil}(\kappa_6)}$$

respectively. This gives us an interval for the solution  $s$ . This gives us a (hopefully small) interval which contains the maximizing  $s$  for the original problem, and we can compute the maximizing  $s$  for the original problem using bisection.

$$\begin{aligned}
\kappa_1 &= -\frac{1}{2}\beta_j^2\Omega^{jj} \\
\kappa_2 &= -\frac{1}{2}\beta_j\sum_{j'\neq j}\frac{\Omega^{jj'}\beta_j}{s_{j'}} \\
\kappa_3 &= \begin{cases} -\frac{1}{2} & \text{SPN} \\ c-1 & \text{SNG} \\ \frac{1+\alpha}{2(1-\alpha)}-1 & \text{SPB} \end{cases} \\
\kappa_4 &= \begin{cases} -\frac{1}{2}\sum_{j'\neq j}\Psi^{jj'}s_{j'} & \text{SPN} \\ 0 & \text{SNG} \\ 0 & \text{SPB} \end{cases} \\
\kappa_5 &= \begin{cases} -\frac{1}{2}\Psi^{jj} & \text{SPN} \\ -c & \text{SNG} \\ -\left(\frac{2\Gamma(\frac{3}{2\alpha})}{\Gamma(\frac{1}{2\alpha})}\right)^{\frac{\alpha}{1-\alpha}}f(\delta_j|\alpha) & \text{SPB} \end{cases} \\
\kappa_6 &= \begin{cases} 2 & \text{SPN} \\ 2 & \text{SNG} \\ \frac{2\alpha}{1-\alpha} & \text{SPB} \end{cases}
\end{aligned}$$

## I.5 Partitioning the Design Matrix $\mathbf{X}$

We recommend partitioning the design matrix as follows:

- Perform an eigendecomposition  $\mathbf{X}'\mathbf{X} = \mathbf{V}\text{diag}\{\mathbf{d}\}\mathbf{V}'$ ;
- Compute the proportion of variance explained by eigenvector  $i$  from  $\pi_i = \frac{d_i}{\sum_{i=1}^p d_i}$  for all of the eigenvalues. Let  $\mathcal{R} = \{1, \dots, p\}$  be the set of indices referring to all of the covariates.
- For  $i = 1 \dots p$ :
  - Select  $k_i = \text{round}(p\pi_i, 0)$  covariates from the indices of remaining covariates  $\mathcal{R}$  with probabilities proportional to  $|\mathbf{v}_{i,\mathcal{R}}|$ .
  - Remove the selected covariates from  $\mathcal{R}$ .

- If  $k_i = 0$  or  $\mathcal{R}$  is empty, set  $m = i$  and break.
- If  $\mathcal{R}$  contains  $r > 0$  indices for  $r$  remaining covariates, split the  $r$  remaining covariates into  $r$  groups of one covariate each.

This yields  $m + r$  partitions of the  $p$  covariates.

## J Hyperparameter Maximum Marginal Likelihood

The marginal likelihood is given by:

$$\int \exp \{ -h(\mathbf{y}|\mathbf{X}, \mathbf{s} \circ \mathbf{z}, \boldsymbol{\phi}) \} \left( \frac{1}{\sqrt{2\pi}|\boldsymbol{\Omega}|} \exp \left\{ -\frac{1}{2} \mathbf{z}' \boldsymbol{\Omega}^{-1} \mathbf{z} \right\} \right) p(\mathbf{s}|\boldsymbol{\theta}) d\mathbf{z} d\mathbf{s}.$$

Given an initial value  $\boldsymbol{\Omega}^{(0)}$ , Gibbs-within-EM estimates of  $\boldsymbol{\Omega}$  can be obtained by iterating the following until  $\|\boldsymbol{\Omega}^{(i+1)} - \boldsymbol{\Omega}^{(i)}\|_F$  converges:

- using MCMC to simulate  $M$  draws  $(\mathbf{z}^{(1)}, \mathbf{s}^{(1)}), \dots, (\mathbf{z}^{(M)}, \mathbf{s}^{(M)})$  from the joint posterior distribution of  $(\mathbf{z}, \mathbf{s})$  given  $\boldsymbol{\Omega}^{(i)}$ ,  $\boldsymbol{\phi}$  and  $\boldsymbol{\theta}$ , set  $\hat{\mathbb{E}}[\mathbf{z}\mathbf{z}'|\boldsymbol{\Omega}^{(i)}, \mathbf{X}, \mathbf{y}, \boldsymbol{\phi}, \boldsymbol{\theta}] = \frac{1}{M} \sum_{j=1}^M \mathbf{z}^{(j)}(\mathbf{z}^{(j)})'$ ;
- set  $\boldsymbol{\Omega}^{(i+1)} = \operatorname{argmin}_{\boldsymbol{\Omega} > 0} \log(|\boldsymbol{\Omega}|) + \frac{1}{2} \operatorname{tr}(\boldsymbol{\Omega}^{-1} \hat{\mathbb{E}}[\mathbf{z}\mathbf{z}'|\boldsymbol{\Omega}^{(i)}, \mathbf{X}, \mathbf{y}, \boldsymbol{\phi}, \boldsymbol{\theta}])$ .

In practice, we will rarely assume  $\boldsymbol{\Omega}$  is unstructured, as doing so requires estimating  $p + p(p-1)/2$  unknown parameters from a single observation of a  $p \times 1$  vector. Instead, we will parametrize  $\boldsymbol{\Omega}$  as a function of lower-dimensional parameters, e.g. as a function of a single autoregressive parameter  $\rho$  or as a function of several separable covariance matrices  $\boldsymbol{\Omega} = \boldsymbol{\Omega}_K \otimes \dots \otimes \boldsymbol{\Omega}_1$  which correspond to variation along different modes of the matrix or tensor of regression coefficients  $\mathbf{B}$ . However, the general approach to maximum marginal likelihood estimation of  $\boldsymbol{\Omega}$  remains the same, with minimization over  $\boldsymbol{\Omega}$  in the second step replaced by minimization over the lower-dimensional components.